CHAPTER 8

STATISTICAL ANALYSIS OF SOFT X-RAY TRANSIENTS

Remember when you were young:
You shone like the sun [...].
Now there's a look in your eyes
Like black holes in the sky.
(Pink Floyd 1975)

8.1. 28 TRANSIENTS

In this final Chapter, keeping in mind all the considerations (and the caveats) made so far in this Thesis and concerning the general homogeneity of the sublcass of SXTs, it has been thought necessary to begin a statistical analysis on the objects belonging to this group. This analysis aims at the detection of the general characteristics of this class and at the evaluation, if possible, of analogies and differences between SXTs and persistent LMXBs. Also, this search will try to pinpoint the features which can help to discern between Type I and Type II SXTs.

This work has been done using the catalog compiled by [200], the IAU circulars published from 1993 to 1996, and refined using the SIMBAD database. Thus, the list of SXTs can be considered updated to the end of December 1996.

The selection criteria used to decide if an object can be considered or not a SXT have been already cited many times in Sect. 3.4; however, here they are again:

- transient X-ray emission: more than 10^{36} - 10^{37} erg s^{-1} or more than 0.1 Crab at maximum light, and around the X-ray satellites sensitivity limit at quiescence;
- a blackbody soft X-ray spectrum with a hard power-law tail during outburst;
- about 1 month of X-ray activity during outburst;

- an optical magnitude jump of more than 4 magnitudes from quiescence to maximum light;

With these criteria, 28 objects which have at least two of the above cited characteristics have been picked out. Twenty of these SXTs are well known and well studied X-ray Novae (and, among them, all the BHXNe); the remaining 8 systems are instead 'forgotten SXTs', in the sense that very little is known of them because they underwent the last outburst not closer than 20 years ago (i.e. during the '70s, when the X-ray astronomy was at its initial stages and it was not possible to get the wealth of information that is available nowadays with the presently flying X-ray satellites) and/or because their optical counterpart is unknown. Thus, the observations of these systems are few and scanty.

Among the selected objects, 27 of them belong to the Galaxy and, according to [200], are classified as LMXBs also in the cases in which the classification is uncertain, thus pointing out that SXTs are a subclass of this group of X-ray binaries.

In the following, the SXTs known to date are presented in increasing right ascension order and briefly described using as a starting point for the best-known systems the collections of data made by [203] and by [190], completed if needed with the quotation of the more recent results. In absence of a known mass function for the compact object, and where not indicated, the transients are classified as Type II SXTs because of their characteristics.

XN SMC 1992 (RX J0117.6-7330). It was discovered [48] from the analysis of archival (October 1992) data of the ROSAT satellite. The likely counterpart is an 14th-magnitude OB star whose optical spectrum shows narrow Balmer emission lines and absorptions lines of He I and N III [38]. This is the only SXT not belonging to the Galaxy and, if the optical counterpart is confirmed, the only one which has an early-type star as a secondary(1).

(1) Recently, Coe et al. (1998; MNRAS, 293, 43) demonstrated that this object is actually a Be-X transient and not a SXT.

V518 Per (GRO J0422+32). This system underwent an outburst starting on August 1992 [154]. It is one of the three SXTs with a basically 'hard' X-ray spectrum [22, 185] and in which the e^--e^+ annihilation line in emission has possibly been detected in the γ-ray spectrum. A transient radio emission has also been detected [175]. Its distance from Earth is about 2 kpc [22, 44]. Superhumps, dips [110] and minioutbursts [44], along with a sharp and episodic drop of the optical luminosity on December 30, 1992 [10] were detected during the decline. Its orbital period is 5.09 hours [44, 45, 110]. The mass function of the primary is only 1.21 $M_{\odot}$ [72], but its mass seems to be around 3.6 $M_{\odot}$; it has thus been classified as a low mass BHXN [72]. The secondary, a Main Sequence M0 - M2 type star [30, 72, 151], probably has lithium in its atmosphere [72]. A further detailed presentation of the observations of V518 Per in outburst and quiescence can be found in [35] and in [78], respectively, as well as in their bibliographic references.

V616 Mon (A0620-00). This is one of the best studied SXTs and it is considered the 'family-founder' of this class of objects, as it has been the first X-ray Nova which has extensively been studied over the whole electromagnetic spectrum, and its outburst behaviour has been assumed as 'typical' for this class, also in the light of the observations subsequently made over other SXTs. This has been the first of these systems to be dynamically classified as a BHC [138]. Its main features are well described in [203] and in [190]. It has a recurrent behaviour [66] and the secondary star shows lithium in its atmosphere [126].

MM Vel (GRS 1009-45). It is one of the 5 SXTs which showed the superhump phenomenon during the active phase [134]. For a thorough description of the object one can see Ch. 5 of this Thesis and references therein. It is a recurrent SXT [62], and it has been defined a 'hybrid' SXT by [134] because of its behaviour similar to both Type I and Type II SXTs.

GU Mus (GRS 1124-68). Also in this case the reader is invited to refer to the description of the characteristics of this SXT made by [203] and [190] and to Ch. 7 of this Thesis (and references therein). It is one of the ‘typical’ BHXNe [32, 153, 164] and it is the only SXT which clearly displayed the presence of the e^--e^+ annihilation line in emission in its γ-ray spectrum during the outburst [77, 184]. In this SXT, too, the presence of lithium on the secondary has been detected [131].

BW Cir (GS 1354-64, Cen X-2?). It is probably associated to the X-ray transient Cen X-2, observed in 1967; it may possibly be a recurrent SXT [76]. For further information, see [190].

V822 Cen (A1455-314, Cen X-4). It is one of the 5 Type I SXTs and the only one for which the mass function of the primary has been determined [139]. It is recurrent [50]; on this subject, see also [203]. The secondary is an evolved and peculiar star [46, 139] and shows the presence of lithium in its atmosphere [130].

KY TrA (A1524-62). The X-ray light curve of this SXT is characterized by an anomalous pre-maximum phase which lasted about one month [105]. After the outburst, occurred in 1974, a restart of the activity has been reported in 1990, even if in X-rays only [9]; it is however not clear whether this X-ray emission came from this object or from another prospectically close to it. For a wider description of this SXT, see [190].

IL Lup (4U 1543-47). It is a recurrent SXT [47, 135]. The optical counterpart is a Main Sequence star of spectral type A1 - A2, probably the outer component of a triple system [40]. For further details, see [190]. The X-ray spectrum shows the Fe K_α line in emission [198].

QX Nor (4U 1608-52). This is the second Type I SXT following the increasing right ascension order. It shows X-ray bursts [162] which allowed such a classification.

It is recurrent [71, 122]; the last outburst occurred on February 1996 [127]. It has detectable quiescent X-ray emission [162] and it has been classified as an 'atoll source'[(2)] [91]. It also displays the Fe K_{α} emission line in its X-ray spectrum [187], and very high freqency QPOs during the outburst [11]. It has a rather faint optical counterpart [85]. A wide description of the characteristics of this SXT can be found in [91] and [122].

Nor X-1 (4U 1630-47). This object is, together with V1333 Aql, one of the two 'periodic' SXTs, in the sense that their outbursts generally occur with quasi-regular intervals, in this case every 600 days [102]. It is however not clear which is the cause of this phenomenon: given the regularity of the recurrence time also after outbursts with different intensity, it has been hypotesized that this behaviour might be referred to an orbital motion [158] or to intrinsic stability mechanisms acting on the secondary [190]. The last X-ray outburst occurred on March 1996 [120]. The optical counterpart has still not been identified [156]. For further information, refer to [190].

XN Sco 1994 (GRO J1655-40). It is a peculiar SXT as, unique in this class, showed (and contines to show, after more than two years after the first eruption) repeated X-ray outbursts very similar among them in shape and intensity [12]; it also has two radio superluminal jets similar to those of AGNs, though on a much smaller scale [93]. Moreover, it is one of the two eclipsing SXTs found to date and the mass function of its primary allowed its classification as BHXN [5]. The reader is invited to refer to Ch. 6 and to its bibliography for the description of the characteristics of this system.

V2107 Oph (1H 1705-25). During the outburst, occurred in 1977 [84], this SXTs showed an unusual 'double maximum' in the X-ray light curve [211]. For a synthesis of the knowledge on this system, see [190]. It should be stressed that this

---

(2) See [197] for the definition of 'atoll source'.

object recently entered the number of BHXNe as it has been spectroscopically determined that the primary has a mass function of 4.0 $M_{\odot}$ [165].

V2293 Oph (GRS 1716-249). It is one of the SXTs with 'hard' X-ray spectrum in outburst [186]. Superhumps have been observed in the optical during the activity phase [133]. A wider description on the behaviour of this SXT during the outburst and the decline phases may be found in Ch. 4 and in its bibliographic references. No quiescent observations on this object are known.

KS 1730-312. This SXT was observed in X-rays, although only for few days, during the outburst occurred on September 1994. In this band, it showed X-ray spectral and light curve behaviours typical of the objects belonging to this class [193]. No optical counterpart is known, as for the bulk of the following SXTs, because of the strong absorption due to the dust placed among the Earth and this object, which is located towards the Galactic Center.

4U 1730-22. Still less is known about this system: it underwent an outburst on August 1972, which was observed only in the X-rays. Further scanty information can be found in [49]. The optical counterpart is unknown.

KS 1731-260. It is a Type I SXT, as it displayed X-ray bursts during an outburst [182]; moreover, it is recurrent [144]. It is located in the direction of the Galactic Center. No optical counterpart has been found.

3U 1735-28. This object instead belongs, like 4U 1730-22, to the group of 'mysterious' SXTs: it underwent an X-ray outburst on March 1971 [75], and only few other things are known [101, 111]. The X-ray spectrum at maximum is however soft [49]. The optical counterpart is, obviously, unkonwn.

GRS 1739-278. Latest discovered SXT, this object was detected for the first time on March 1996, but according to [83] the outburst may have started on November 1995. Again according to these authors, the system may be similar to GRS 1915+105. The optical counterpart, a heavily reddened object, shows a not particularly strong H_α emission line [142].

1H 1741-322. Very little is known about this object: the only known outburst occurred on August 1977 and it has been observed in the X-rays only; the optical counterpart is unknown [177]. Other sparse information can be found in [190] and in [200].

A1742-289. Type I SXT (it has been detected the presence of X-ray bursts during quiescence [125]), it shows X-ray eclipses at quiescence which allowed the measurement of its orbital period [125]. Its optical counterpart is practically invisible due to the strong absorption of the big amount of interstellar dust along the line of sight: probably the secondary is a G-type Main Sequence star [125]. This system is located in the direction of the Galactic Center. Further information is available in [125] and references therein. However, see note (1) of Ch. 5 for different conclusions on the nature of the primary in this SXT.

A1744-361. The most 'mysterious' SXT: the only source of information is [57]. Clearly, the optical counterpart is not known and it is also not possible to say whether this is a LMXB or a MXRB [200], nor it is possible to make any conjecture on the nature of the compact object.

MX 1746-20. Unique case among SXT, this object is placed in a globular cluster, NGC 6440. The few remaining information can be found in [92]. Also in this case it is not possible to state which is the Type of this SXT.

2S 1803-245. This SXT displayed an outburst on May 1976 [99]. Very little else is known but the fact that the optical counterpart is unknown and that also in this case it is unclear whether this object is a LMXB or a MXRB [200]; nor it is known which Type of SXT this object belongs to.

EXO 1846-031. This object was observed only in the X-ray band and its optical counterpart was not found [157]; see also [190]. The few X-ray known characteristics allowed its classification as a Type II SXT.

V1333 Aql (4U 1908+00, Aql X-1). Fifth and, for the moment, last SXT containing a NS (the X-ray bursts of which were revealed during an outburst occurred in 1979 [116]), this is the other 'periodic' X-ray Nova: indeed it shows outbursts, with strongly variable peak intensity, with a periodicity of about 435 days. See also [203].

QZ Vul (GS 2000+25). Together with V616 Mon and GU Mus, this is one of the 'classic' SXTs, because its behaviour in outburst and quiescence reflects the 'canonical' one for this kind of objects. The summary of its activity during outburst can be found in [190]; besides, the determination of the mass function of the collapsed object (which is about 5 $M_{\odot}$) allowed stating that QZ Vul is the second best BHC of the class and of the whole Galaxy [31, 73]. Moreover, the optical spectra taken at quiescence allowed the detection of lithium on the secondary star [73, 87].

V404 Cyg (GS 2023+338). Third 'hard' SXT, it is the best BHC of the Galaxy: it indeed has a mass function of the primary of about 6 $M_{\odot}$, which leads to state that the compact object is a BH beyond any reasionable doubt [26]. Also in this case, a detailed description of this system is available in [190] and in [203]. Moreover, its quiescent X-ray spectrum shows the presence of the Fe K_{α} line in emission [150], while the optical spectra reveals here, too (it was the first all-time detection among SXTs), the presence of lithium on the secondary [129, 209]. It is recurrent [166, 206].

The objects EU 1737-132, 1741.2-2859 e 1918+146 were excluded from this list because the information on them is very poor [200], so it is neither possible to classify them as SXTs nor, on the contrary, state that they do not surely belong to this group of systems. To these objects one can add the Classical Novae KT Mon, CT Ser e Q Cyg which, according to [35], showed an outburst optical behaviour very similar to that typical of SXTs, but exploded before the X-ray astronomy was born.

Table 8.I resumes the main characteristics of each SXT. In the following a wide column-by-column description of the Table will be given. When no bibligraphic citation is indicated, this means that the value has been computed in the framework of this Chapter using already published values and formulae.

The first two columns report equatorial at the epoch J2000.0 (when known at epoch B1950.0, their precession to equinox J2000 was computed), while columns 3 and 4 report the corresponding galactic coordinates l^{II} e b^{II}, evaluated by means of appropriate conversion formulae. Columns 5 contains the date of the last outburst and column 6 lists the year(s) of the previous outburst(s), if any, or the recurrence time of the SXT. Column 7 gives the X-ray peak flux in Crab units; "var." indicates (only for recurrent SXTs) that this value varies from outburst to outburst. Columns 8, 9 and 10 respectively report if X-ray bursts, X-ray flickering and QPO (with their frequency in mHz) were observed.

Column 11 gives the *V* magnitude (or other optical band where indicated) at light peak; column 12 lists the L_X/L_{opt} ratio, corrected for interstellar absorption, at maximum light (or simply the X-ray luminosity at maximum if the optical counterpart is not known): in the cases in which the peak X-ray luminosity is not known, it was computed on the basis of the peak X-ray flux by means of the relation

$$L_x = 4\pi d^2 F_x \quad , \tag{8.1}$$

where *d* (in cm) is the distance to the SXT (column 17). As it can be seen in column 12, in some cases the value of *d* (in kpc; the number at the foot indicates the distance estimate used in the expression) has been left indicated, when it is not known exactly.

Table 8.I. Main properties of SXTs in outburst and at quiescence. See text for the meaning of each column.

	1	2	3	4	5	6
NAME	α (2000)	δ (2000)	l^{II}	b^{II}	Date of last outburst	Previous outbursts
XN SMC 1992 (RX J0117.6-7330)	$01^h 17^m 41^s.9$ [48]	-73° 31' 01" [48]	300°.4	-43°.5	1/10/1992 [48]	
V518 Per (GRO J0422+32)	$04^h 21^m 42^s.75$ [34]	+32° 54' 26".8 [34]	165°.9	-11°.9	5/8/1992 [154]	
V616 Mon (A0620-00)	$06^h 22^m 44^s.5$ [14]	-00° 20' 44" [14]	210°.0	-6°.5	3/8/1975 [69]	1917 [66]
MM Vel (GRS 1009-45)	$10^h 13^m 36^s$ [59]	-45° 04' 35" [59]	275°.9	+9.3	12/9/1993 [119]	1982 [62]
GU Mus (GRS 1124-68)	$11^h 26^m 26^s.62$ [60]	-68° 40' 32".5 [60]	295°.3	-7°.0	8/1/1991 [60]	
BW Cir (Cen X-2?, GS 1354-64)	$13^h 50^m 09^s.6$ [113]	-64° 44' 05" [113]	310°.0	-2°.8	13/2/1987 [113]	1967 ? [76]
V822 Cen (Cen X-4)	$14^h 58^m 21^s.9$ [25]	-31° 40' 07" [25]	332°.2	+23°.9	11/5/1979 [25]	1969 [50]
KY TrA (A1524-62)	$15^h 28^m 16^s.5$ [146]	-61° 52' 58" [146]	320°.3	-4°.4	27/8/1990 ? [9]	1974 [105]
IL Lup (4U 1543-47)	$15^h 47^m 08^s.5$ [47]	-47° 40' 09" [47]	330°.9	+5°.4	18/4/1992 [88]	1971 [135] 1983 [47]
QX Nor (4U 1608-52)	$16^h 12^m 42^s.9$ [85]	-52° 25' 23" [85]	330°.9	-0°.9	23/2/1996 [127]	'70 (2), '71 (2), '75, '77, '79 [71, 122]
4U 1630-47 (Nor X-1)	$16^h 34^m 00^s.3$ [156]	-47° 23' 39" [156]	336°.9	+0°.3	20/3/1996 [120]	recurs every ~615 days [102]
XN Sco 1994 (GRO J1655-40)	$16^h 54^m 00^s.137$ [4]	-39° 50' 44".9 [4]	345°.0	+2°.5	27/7/1994 [90]	
V2107 Oph (1H 1705-25)	$17^h 08^m 14^s.5$ [84]	-25° 05' 29" [84]	358°.6	+9°.1	8/8/1977 [84]	
V2293 Oph (GRS 1716-249)	$17^h 19^m 36^s.87$ [61]	-25° 01' 03".4 [61]	0°.1	+7°.0	25/9/1993 [61]	
KS 1730-312	$17^h 33^m 27^s.88$ [193]	-31° 12' 56".8 [193]	356°.6	+1°.0	23/9/1994 [18]	
4U 1730-22	$17^h 33^m 56^s.55$ [200]	-22° 02' 07".2 [200]	4°.5	+5°.9	8/1972 [49] (Fig. 1*b*)	
KS 1731-260	$17^h 34^m 12^s.9$ [181]	-26° 05' 10" [181]	1°.1	+3°.7	7/1996 [144]	1989 [182]
3U 1735-28	$17^h 38^m 33^s.77$ [75]	-28° 28' 40".5 [75]	359°.6	+1°.6	11/3/1971 [111]	
GRS 1739-278	$17^h 42^m 40^s.3$ [83]	-27° 44' 54" [83]	0°.7	+1°.2	11/1995 ? [83]	
1H 1741-322	$17^h 45^m 01^s.72$ [200]	-32° 13' 37".5 [200]	357°.1	-1°.6	19/8/1977 [104]	
A1742-289	$17^h 45^m 36^s.9$ [147]	-29° 01' 07" [147]	359°.9	0°.0	15/2/1975 [70] (Fig. 1)	
A1744-361	$17^h 48^m 13^s.3$ [200]	-36° 07' 53" [200]	354°.1	-4°.2	1/3/1976 [57]	
MX 1746-20	$17^m 48^m 53^m.4$ [92]	-20° 22' 02" [92]	7°.7	+3°.8	12/1971 [74]	
2S 1803-245	$18^h 06^m 50^s.1$ [99]	-24° 35' 15" [99]	6°.1	-1°.9	5/5/1976 [99]	
EXO 1846-031	$18^h 49^m 16^s.9$ [157]	-03° 03' 53" [157]	29°.9	-0°.9	3/4/1985 [157]	
V1333 Aql (Aql X-1)	$19^h 11^m 15^s.9$ [191]	+00° 35' 06" [191]	35°.7	-4°.1	29/5/1996 [97]	recurs every ~435 days [107]
QZ Vul (GS 2000+25)	$20^h 02^m 49^s.49$ [194]	+25° 14' 11".2 [194]	63°.4	-3°.0	26/4/1988 [194]	
V404 Cyg (GS 2023+338)	$20^h 24^m 03^s.7$ [112]	+33° 52' 04" [112]	73°.1	-2°.1	2/5/1989 [112]	1938 [206] 1956, 1979 ? [166]

Column 13 reports if the object showed a transient radio emission, while columns 14 and 15 list the references where X-ray and optical spectra at maximum are reported.

Table 8.I. (continued)

	7	8	9	10	11	12
NAME	X-ray maximum (Crab)	X-ray bursts	X-ray flickering	QPO (mHz)	V_{max}	L_X/L_{opt} or L_X (erg s^{-1}) at maximum
XN SMC 1992 (RX J0117.6-7330)	≥ 0.004					$L_X \geq 2.5 \cdot 10^{37}$ [48]
V518 Per (GRO J0422+32)	3 [22]		YES [205, 175]	~30 [168] ~300 [205]	12.6 [33]	≈44 [44]
V616 Mon (A0620-00)	~50 [64]				11.2 [212]	~2000 [212]
MM Vel (GRS 1009-45)	~0.8 [119]		YES [119]		≅ 13.85 [134]	≈500 (from [62])
GU Mus (GRS 1124-68)	~8 (1÷6 keV) [114] 2.2 (8÷20 keV) [118]		YES [68]	3 to 10 [190]	≅ 13.3 [60]	≥100 [60]
BW Cir (Cen X-2?, GS 1354-64)	~0.13 [113]				16.92 [113]	~300
V822 Cen (Cen X-4)	~20 (1969) [50] ~4 (1979) [25]	YES [137]			12.8 [25]	300 [53]
KY TrA (A1524-62)	0.9 [105]				17.5 (*B*) [146]	≤ 200 [146]
IL Lup (4U 1543-47)	~2 (var.) [121]				14.9 [161]	~1700
QX Nor (4U 1608-52)	~1.1 (var.) [85]	YES [162]		$\sim 8.5 \cdot 10^5$ [11]	<18.2 (*I*) [85]	≤ 200 [85]
4U 1630-47 (Nor X-1)	~0.5 (var.) [156]		YES [156]			$L_X \sim 3 \cdot 10^{38} \cdot d^2_{10}$ [156]
XN Sco 1994 (GRO J1655-40)	1.1 [216]		YES [82]		14.0 [4] (Fig. 3)	≈150
V2107 Oph (1H 1705-25)	~3.5 [211]				16.5 (*B*) [84]	~100 [84]
V2293 Oph (GRS 1716-249)	1.4 [89]			~40 to ~300 [196]	≈16.3 [61]	≈1400 [61]
KS 1730-312	0.5 [18]					$L_X \sim 2.2 \cdot 10^{38}$ [193]
4U 1730-22	0.1 [49]					$L_X \sim 3 \cdot 10^{36} \cdot d^2_{10}$ [178]
KS 1731-260	~0.2 (var.) [144, 182]	YES [182]				$L_X \sim 1.5 \cdot 10^{37}$ [179]
3U 1735-28	~0.4 [75]					$L_X \sim 4 \cdot 10^{37}$ [75]
GRS 1739-278	≥0.5 ? [83]				20.5 (*R*) [142]	$L_X \sim 1.6 \cdot 10^{40} \cdot d^2_7$ [83]
1H 1741-322	~0.7 [177]					$L_X \sim 2 \cdot 10^{38} \cdot d^2_{10}$
A1742-289	~1.8 [70]	YES [125]				$L_X \sim 7 \cdot 10^{36}$ [147] $L_X \sim 3 \cdot 10^{38}$ [21]
A1744-361	0.25 [57]					$L_X \sim 2 \cdot 10^{36} \cdot d^2_{10}$ [178]
MX 1746-20	~0.15 [74]					$L_X \sim 2 \cdot 10^{37} \cdot d^2_7$ [178]
2S 1803-245	~0.8 [99]					$L_X \sim 2 \cdot 10^{37} \cdot d^2_{10}$ [178]
EXO 1846-031	~0.3 [157]					$L_X \sim 10^{38}$ [157]
V1333 Aql (Aql X-1)	~1.3 (var.) [36]	YES [116]	YES [36]		14.8 [36]	~200 [36]
QZ Vul (GS 2000+25)	12 [194]		YES [189]		16.4 [37]	~2000 [37,194]
V404 Cyg (GS 2023+338)	~21 [189]		YES [143]	2 - 6 [79, 207]	11.7 [103]	~15 [29]

Column 16 gives the color excess *E(B-V)*; in the cases in which it is not known, it was evaluated from the relation in [163] between it and the hydrogen column density

Table 8.I. (continued)

	13	14	15	16	17	18	19
NAME	Radio emission	Outburst X-ray spectrum	Outburst optical spectrum	*E*(*B-V*)	*d* (kpc)	$\mid z \mid$ (pc)	M_V^{max}
XN SMC 1992 (RX J0117.6-7330)					~50 [190]		
V518 Per (GRO J0422+32)	YES [175]	[185]	[175]	0.4 [44]	1 - 2 [22] 2 [44]	200 - 400	+0.5 [44]
V616 Mon (A0620-00)	YES [56, 212]	[167]	[149, 212]	0.4 [212]	0.87 [148] 1.05 [171]	70 [214]	+0.7 [201]
MM Vel (GRS 1009-45)		[186]	[62]	0.2 [62]	1.5 - 4.5 [62]	200 - 700	0 - +2.5 [62] (Fig. 9)
GU Mus (GRS 1124-68)	YES [6]	[68, 81, 114]	[60, 63]	0.3 [60]	~5.5 [153] ~8 [39]	~600	≈ -1
BW Cir (Cen X-2?, GS 1354-64)				~1 [113]	10 ? [113]	< 500	≈ -1
V822 Cen (Cen X-4)	YES [94]	[19]	[25]	0.1 [13]	1.2 [46]	~400	+1.5 [201]
KY TrA (A1524-62)				0.7 [202]	4.4 [202]	350 [214]	> +1 - +2 (*B*) [146]
IL Lup (4U 1543-47)		[47, 198]	[161]	0.7 [40]	~4 [40]	340 [214]	≈0; or ~ +1.5 [40]
QX Nor (4U 1608-52)				1.5 [200]	≤ 3 [162]	< 50	
4U 1630-47 (Nor X-1)		[156, 158]		4.5 [200] 2 - 20 [158]	~10 [156]	~50	
XN Sco 1994 (GRO J1655-40)	YES [90, 93]	[90]	[4, 12]	1.15 [4]	3.2 [93]	120	≈ -2 [4]
V2107 Oph (1H 1705-25)		[51]	[84]	~0.5 [84]	~3 [84] ~6 [165]	~500	≈ +0.5
V2293 Oph (GRS 1716-249)	YES [61]	[186]	[61]	0.9 [61]	2 - 2.8 [61]	~300	+1.5
KS 1730-312		[18, 193]		~12 (from [18])	8.5 (assumed) [18]	~250	
4U 1730-22							
KS 1731-260		[182]		3.2 [200]	8.5 (assumed) [179]	~550	
3U 1735-28					6.3 [214]	180 [214]	
GRS 1739-278	YES [65, 96]			~4.5 (from [83])	6 - 8.5 [83]	~150	
1H 1741-322		[51]					
A1742-289	YES [55]	[21]		~50 (from [125])	~10 [125]	0 [214]	
A1744-361							
MX 1746-20				1.17 [132]	5.8 [132]	380	
2S 1803-245							
EXO 1846-031		[157]		~6 (from [157])	~7 [157]	~100	
V1333 Aql (Aql X-1)	YES [95]		[36]	0.37 [191]	1.7 - 4.0 [191]	120 - 300	+0.9 [201]
QZ Vul (GS 2000+25)	YES [94]	[180, 194]	[37]	1.69 [37]	~2 [24, 87]	~100	~ -1 [37]
V404 Cyg (GS 2023+338)	YES [86]	[112, 183]	[27, 207]	1.03 [207]	3.5 [208] ~2.6 [29]	100 - 150	-4.7 [201]

along the line of sight

$$N_{\rm H} = 1.79 \cdot 10^{21} A_V = 5.55 \cdot 10^{21} E(B-V) \quad , \qquad (8.2)$$

in which A_V is the absorption (expressed in magnitudes) in the *V* band.

Table 8.I. (continued)

	20	21	22	23	24	25
NAME	P_{sh} (hr)	Dips and/or eclipses	Short-term periods or oscillations	*e*-fold decay time in X-rays (days)	d*V*/dt (mag d^{-1})	Times of secondary maxima (days)
XN SMC 1992 (RX J0117.6-7330)			[48]	~44 [48]		
V518 Per (GRO J0422+32)	5.18 [110]	dips [110]		44 [205]	0.0085 [44]	every ~120 [44]
V616 Mon (A0620-00)	8.14 ? [218]			28.9 [106]	~0.015 [212]	~60 and ~180 [212] (Fig. 2)
MM Vel (GRS 1009-45)	4.79 [134]		[3]	~10 [119, 134]	0.0147 [134]	~30 (X) [155], ~90 [134, 155], ~170 [3]
GU Mus (GRS 1124-68)	10.54 [2]			31.2 [114]	0.024 [60]	~80 [63, 114] ~200 [63, 68]
BW Cir (Cen X-2?, GS 1354-64)				~66 [113]		
V822 Cen (Cen X-4)				≈3 [108]	0.12 [25]	~5 and ~11 [25] (Fig. 2)
KY TrA (A1524-62)				52 [146]	0.0085 [146]	
IL Lup (4U 1543-47)				~50 - 70 [141]		~80 [121]
QX Nor (4U 1608-52)			[145]	~10 or ~70 [122]		
4U 1630-47 (Nor X-1)			in X at max. [156]	~50 [156]		
XN Sco 1994 (GRO J1655-40)		eclipses [4]			≈0.016 [78]	X: every ~120 [217]; opt: ~80, ~320 [78] (Fig. 9)
V2107 Oph (1H 1705-25)				~60 - 90 [211]		~30 (X) [213]
V2293 Oph (GRS 1716-249)	14.7 [133]		[133]	≈300 [89]	≥ 0.0082 [133]	X: ~50 [196] (Fig. 1), ~330 [16]; opt: ~480 [17, 109, 133]
KS 1730-312						
4U 1730-22				≈30 [49]		~40 (X, probable) [49] (Fig. 1*b*)
KS 1731-260				~10 [182] (Fig. 2)		
3U 1735-28						
GRS 1739-278						~90 (X) ?, ~120 (X) ? [83]
1H 1741-322						
A1742-289		ecl. X [125]		~12 [147]		~40 [21]
A1744-361						
MX 1746-20						
2S 1803-245						
EXO 1846-031				~84 (3÷6 keV); ~30 (6÷10 keV) [157]		
V1333 Aql (Aql X-1)			[170]	~30 [107]	~0.022 [124] (Fig. 2)	
QZ Vul (GS 2000+25)	8.33 [37]		[41]	30.8 [194]	0.016 [159]	~70 (X) [194] ~170 [159]
V404 Cyg (GS 2023+338)			[160]	~40 [189]	0.0094 [78]	~120 [86] (Fig. 12)

Column 17 lists the distances to the systems in kpc, while column 18 reports the height z (in pc) on the Galactic Plane. The latter has been evaluated, in absence of bibliographic indications, from the formula

Table 8.I. (continued)

	26	27	28	29	30	31	32
NAME	Mini-outbursts	Decline X-ray spectrum	Decline optical spectrum	$V_{\rm min}$	Δm (*V*)	M_V^{min}	L_X (erg s^{-1}) at quiescence
XN SMC 1992 (RX J0117.6-7330)				14.2 ? [38]		-4.6 [38]	
V518 Per (GRO J0422+32)	YES [44]	[199]	[22]	~22 [45]	~9.5	~ +10 [23]	
V616 Mon (A0620-00)		[123]	[149, 212]	~18.3 [147]	~7.1	+8.0 [148]	~$6 \cdot 10^{30}$ [140]
MM Vel (GRS 1009-45)	YES [3]		[3, 134]	>22 [134]	>8 [134]	≥ +6.5 (*B*) [62]	
GU Mus (GRS 1124-68)		[68, 81, 114]	[63]	~20.5 [58]	≈7.2 (from [58])	~ +6 [153]	
BW Cir (Cen X-2?, GS 1354-64)		[113]	[52]	~22 (*R*) [113]	~5 (from [113])	≥ +4 (from [113])	
V822 Cen (Cen X-4)		[137]		~18.5 [46]	~6 [46]	~ +8 [139]	~$8 \cdot 10^{32}$ [204]
KY TrA (A1524-62)		[7] (quiescence)		>21 (*TV*) [146]	>3.5 [146]	> +6 (*B*) [146]	<$2 \cdot 10^{33}$ [9]
IL Lup (4U 1543-47)				16.7 [40]	1.8 [40]	≈ +2 or ≈ +3.5	
QX Nor (4U 1608-52)		[187, 215] (quiescence)		>20 (*I*) [85]	>1.8 (*I*) [85]		~$1.9 \cdot 10^{33}$ [1]
4U 1630-47 (Nor X-1)		[156]					
XN Sco 1994 (GRO J1655-40)			[5, 12]	17.3 [4]	3.3 [90]	≈ +1 (from [4])	
V2107 Oph (1H 1705-25)		[213]		~21.5 [165]	~5.2 (from [165])	≈ +6	<$5 \cdot 10^{32}$ [204]
V2293 Oph (GRS 1716-249)	YES [109, 133]		[133]	≥21 [61]	≥4.4 [61]	> +6	
KS 1730-312							
4U 1730-22							
KS 1731-260		[8] (quiescence)					
3U 1735-28		[101] (quiescence)					
GRS 1739-278							
1H 1741-322		[51]					
A1742-289		[21, 125]					~10^{35} [125]
A1744-361							
MX 1746-20							~10^{33} [100]
2S 1803-245							
EXO 1846-031		[157]					
V1333 Aql (Aql X-1)			[191] (quiescence)	19.17 [191]	~4.4	~ +5.5	~10^{33} [204]
QZ Vul (GS 2000+25)	YES [41]		[15]	>21 (*B*) [194]	>3.5 (*B*) [194]	+5.4 - +6.7 [41]	<10^{31} [204]
V404 Cyg (GS 2023+338)		[183]	[27, 80]	19.2 [188]	7.5 [195]	+2.5 [208]	~$1.5 \cdot 10^{33}$ [204]

$$z = d_{\rm pc} \, {\rm sen}\, b^{\rm II} \quad ; \qquad (8.3)$$

column 19 lists the absolute magnitude at maximum in the *V* or in other optical bands where indicated. When not known in literature, it has been computed here by means

Table 8.I. (continued)

	33	34	35	36	37	38	39	40	41
NAME	P_{orb} (hr)	$f(M_1)$ ($M_\odot$)	i (°)	q	M_1 ($M_\odot$)	M_2 ($M_\odot$)	a ($R_\odot$)	R_{L1} ($R_\odot$)	R_{L2} ($R_\odot$)
XN SMC 1992 (RX J0117.6-7330)									
V518 Per (GRO J0422+32)	5.09 [44, 45, 110]	1.21 [72]	41 [30] ≤45 [23]	0.1093 [72]	3.57 [72] ≥3.4 [23]	0.39 [72]	2.37 [72]	1.1	0.5 [72]
V616 Mon (A0620-00)	7.75 [138]	3.18 [138]	31 - 54 [171]	0.067 [126]	10 [171]	0.6 [171]	4.3 [171]	1.9	0.8
MM Vel (GRS 1009-45)	6.86 [174]		37 - 80 [174]		>1.6 ? [134]	~0.5 ? [134]			
GU Mus (GRS 1124-68)	10.38 [153]	3.01 [153] 3.34 [32]	54 - 65 [153]	0.133 [152] 0.128 [32]	5.92 [164]	~0.7 [164]	4 - 5 [164]	~2	~1
BW Cir (Cen X-2?, GS 1354-64)	~46 ? [98]								
V822 Cen (Cen X-4)	15.1 [46]	0.2 [139]	≈35 - 40 [139]	~0.067 [139]	~1.4 [139]	~0.1 [139]	3.54	1.6	0.65
KY TrA (A1524-62)									
IL Lup (4U 1543-47)									
QX Nor (4U 1608-52)	98.4 ?, 124.6 ? [122]		~60 [67]		~1.4 [67]				
4U 1630-47 (Nor X-1)									
XN Sco 1994 (GRO J1655-40)	62.4 [5]	3.16 [5]	85 [5]	≤0.28 (from [5])	5.4 [5]	≤1.5 [5]	≤15.2	~6.5	≤4.3
V2107 Oph (1H 1705-25)	12.5 [165] 16.8 [128]	4.0 [165]	60 - 80 [165]	≤0.2 [128]	6 [165]	~0.75 [165]	~5	~2.3	~1
V2293 Oph (GRS 1716-249)					>4.9 ? [133]				
KS 1730-312									
4U 1730-22									
KS 1731-260									
3U 1735-28									
GRS 1739-278									
1H 1741-322									
A1742-289	8.36 [125]		~70 [125]	≤0.8 [125]	~1.4 [125]	~1 [125]	~2.7 [125]	~1.10	~0.95
A1744-361									
MX 1746-20									
2S 1803-245									
EXO 1846-031									
V1333 Aql (Aql X-1)	19.0 [42]		≈33 [54]		~1.4 (from [116])				
QZ Vul (GS 2000+25)	8.26 [43]	4.97 [73] 5.02 [31]	65 [24]	0.05 [73] 0.042 [87]	8.5 [24]	0.4 - 0.7 [73]	~4	~2	≤0.85 [73]
V404 Cyg (GS 2023+338)	155.4 [28]	6.08 [26]	56 [172]	0.06 [26]	10 [173] ≤12.5 [169]	0.7 [172]	34 [172]	15.4	~7 [208]

of the distance modulus, using d (in pc) and the apparent magnitude at light maximum corrected for the interstellar absorption:

$$\mathrm{M} - \mathrm{m} = 5 - 5 \,\mathrm{Log}\, d_{\mathrm{pc}} \quad . \tag{8.4}$$

Table 8.I. (continued)

	42	43	44	45	46	47
NAME	Secondary spectral type	Lithium on the secondary	Systemic γ velocity (km s^{-1})	Corr. γ vel. (km s^{-1})	Comments and notes	Result
XN SMC 1992 (RX J0117.6-7330)	OB? [48]				SXT with high-mass companion? [48]	BH?
V518 Per (GRO J0422+32)	M0 V [151] M2 V [30, 72]	? [72]	+9.2 [72]		Hard X-ray spectrum [22]; e^--e^+ annihil. line? [168]; fading episode on 30/12/1992 [10]	BH
V616 Mon (A0620-00)	K4 - K7 V [148, 171]	YES [126]	+10 [152]	-15 [20]	Claimed $7^d.8$ long-term periodicity [136]; occasional short (0.5 - 5 ms) flashes [176]	BH
MM Vel (GRS 1009-45)	K V [134, 174]				Long (~1 month) plateau in X-ray light curve [119]	BH?
GU Mus (GRS 1124-68)	K3 - K4 V [32]	YES [131]	+16 [153] +19.5 [32]	+26 [20]	e^--e^+ annihil. line [77, 184]; local min. in the 8÷20 keV band ~10 days after outburst [118]	BH
BW Cir (Cen X-2?, GS 1354-64)			+15 ? [52]		Position consistent with the X-ray transient Cen X-2 [200]	BH?
V822 Cen (Cen X-4)	K7 V [46]	YES [130]	+137 [139]		Possible $8^h.2$ period in X-rays [108, 117]; peculiar evolved low-mass secondary [46, 139]	NS
KY TrA (A1524-62)					Long (~1 month) X-ray pre-maximum [105]; hard X-ray spectrum [105]	BH?
IL Lup (4U 1543-47)	A1 - A2 V [40]				Triple system? [40]; iron K_α emission line [198]	BH?
QX Nor (4U 1608-52)	K V ? [122]				Bimodal outbursts [122]; atoll source [91]; iron K_α emission [187]; X-ray persistent [162]	NS
4U 1630-47 (Nor X-1)					Unknown optical counterpart	BH?
XN Sco 1994 (GRO J1655-40)	F5 IV [5]		-150 [20]	-114 [20]	Several maxima in X-rays [4]; superluminal radio jets [93, 192]; superhumps? [5]	BH
V2107 Oph (1H 1705-25)	K3 V [165]		+10 [165]	+38 [20]	Double-peaked X-ray maximum [211]	BH
V2293 Oph (GRS 1716-249)	late K ? [61]				Hard X-ray spectrum [186]	BH?
KS 1730-312					Unknown optical counterpart	BH?
4U 1730-22					Unknown optical counterpart	BH?
KS 1731-260					Unknown optical counterpart	NS
3U 1735-28					Unknown optical counterpart	BH?
GRS 1739-278					No strong H_α emission line at maximum [142]; possibly similar to GRS 1915+105 [83]	BH?
1H 1741-322					Unknown optical counterpart	BH?
A1742-289	G V ? [125]				Possible plateau in X-ray light curve [21]; optical counterpart practically invisible [125]	NS
A1744-361					Unknown optical counterpart; uncertain if LMXB or MXRB [200]	?
MX 1746-20					Inside the globular cluster NGC 6440 [92]	?
2S 1803-245					Unknown optical counterpart; uncertain if LMXB or MXRB [200]	?
EXO 1846-031					No optical counterpart found [157]	BH?
V1333 Aql (Aql X-1)	K0 V [191]				Possible 'mild' outbursts [42]; $1^d.3$ periodicity in X? [210]; doubts on recurrence time [115]	NS
QZ Vul (GS 2000+25)	K5 V [31] K3 - K6 V [87]	YES [73, 87]	+18.9 [87]		$10^h.02$ periodicity present (starspots?) [43]	BH
V404 Cyg (GS 2023+338)	K0 IV [166]	YES [129, 209]	-0.4 [26]	+8.5 [20]	Local minimum ~5 days after max. [207]; hard X-ray spectrum [189]; Fe K_α emiss. line [150]	BH!

In column 20 the period of the superhump phenomenon, if observed, is given, while columns 21 and 22, respectively, report if the presence of dips or eclipses and of short-term oscillations (such as, e.g., pulses), different from superhump or orbital (in column 33) origin, has been detected. Column 23 gives the X-ray light curve *e*-folding times $\tau_{1/e}$ expressed in days, and column 24 the optical decline rates (in mag d^{-1}) in the V band, or in other bands if indicated. In column 25 the times of secondary and tertiary maxima of the X-ray and/or the optical light curve are reported and expressed in days from the beginning of the outburst; column 26 indicates if optical minioutbursts took place in the late decline. Column 27 and 28 respectively list the papers in which the decline X-ray and optical spectra are reported; column 29 gives the quiescent V magnitude (or in other bands if indicated), column 30 the full amplitude of the outburst in the V or other optical bands and column 31 the absolute optical magnitude at minimum computed, when not known, using Eq. (8.4). Column 32 instead reports the X-ray luminosity at quiescence.

Columns 33 to 41 contain fundamental orbital parameters for these systems, that is, in order, the orbital period in hours, the mass function in expressed in $M_{\odot}$, the inclination in degrees, the mass ratio, the masses of primary and secondary stars (again in $M_{\odot}$), the orbital separation in $R_{\odot}$ and computed, if not known, using Kepler's third law, and the Roche lobe radii (in $R_{\odot}$) of the components evaluated with Eq. (1.9) if not known.

In column 42 the spectral type of the secondary star is reported; column 43 indicates if lithium is present in the atmosphere of the secondary. Column 44 and 45 give the γ-velocities of the barycenter of these systems with respect to the Sun and the same quantities corrected for the Galactic rotation, respectively. Column 46 reports peculiarities and comments for each SXT and, finally, column 47 classifies the compact object.

All these data will now be analyzed, in order to search for possible correlations hidden among them. The aim is then to find out the general statistical, X-ray and optical properties of outbursting and quiescent SXTs, and to stress the differences between the behaviours of Type I and Type II SXTs. Let us now investigate the properties of this subclass of LMXBs, with particular attention to the possible cross-correlations among the quantities reported in Table 8.I.

8.2. STATISTICAL PROPERTIES OF SXTs

Objects which can be classified as SXTs with an acceptable degree of confidence are thus 28: of them, 5 (i.e. 18%) are Type I SXTs; 20, that is 71%, are Type II SXTs (and, among them, 7 are spectroscopically confirmed BHCs). Only 3 objects (11% of the class members) cannot be classified due to the poor knowledge of their characteristics. Therefore, it is clear the high incidence (more than 2/3 of the total number of objects) of possible BHs in this subclass of SXTs.

The galactic distribution of SXTs seems to follow that of LMXBs; this would confirm that the systems analized here do belong to this class of X-ray binaries. For instance, SXTs have a mean galactic latitude $<b^{II}> = 0°.9 \pm 6°.6$, in agreement with that of LMXBs [219]. Clearly, XN SMC 1992 has been excluded from this computation because it does not belong to the Galaxy. Then, one can note that SXTs group toward the Galactic Bulge (Fig. 3.2), thus indicating a quite old stellar population (see Ch. 3). Indeed (see column 42 of Table 8.I), the secondaries of SXTs are generally late type Main Sequence, or in some cases evolved, stars. The only two systems which do not have a mid- or late-type secondary star are XN SMC 1992 [48] and IL Lup [40]. For the latter case it has been hypothesized that the optical counterpart actually observed is either an interloper star, prospectically superimposed to the system or, more likely, the outer component of a triple system in which the two inner bodies are the real responsible of the transient X-ray activity [40]. XN SMC 1992, instead, is a stand-alone: first of all, its optical counterpart is still not firmly established [48]; secondly, it belongs to another galaxy, that is the Small Magellanic Cloud [38], which could bear some source of diversity.

Thus, one can ask why SXTs seems to take place only amongst LMXBs and none of them is found in MXRBs, at least in the Galaxy. To produce SXTs one needs disks (that is, Roche lobe overflow) which undergo periodic instability phases, and these instabilities can occur only if $\dot{M}$ is relatively low [220]. This is possible only if the primary compact object is more massive than the secondary (see Sect. 3.3); therefore, if one wants SXTs in MXRBs (which are known to have rather massive OB type secondaries), one should have as primaries BHs with masses larger than 30 - 40 $M_{\odot}$, which is quite unlikely. The only reasonable alternative is that of a Be-X system with a BH; in this system the transient behaviour is due no more to disk instability (the disk would not form because of what explained in Ch. 1) but rather to the elliptical orbit of the primary. This possibility also is however unlikely because the eccentricity of the orbit of compact components in MXRBs depends on the mass of the supernova ejecta [221]. Since almost all the mass of the parent supernova is not ejected but collapses into the singularity of the BH [221], the orbit of the compact object should not become very eccentric and should be instead rapidly circularized by the gravitational radiation losses [221]. Indeed, as one can note in column 44 of Table 8.I, the systemic velocity of the system (likely connected to the supernova explosion) appears to be higher in Cen X-4, which is known to contain a NS, rather than in Type II SXTs; the exception to this rule is GRO J1655-40, whose genesis is discussed by [20].

To all these considerations it must be added that the more massive secondaries of MXRBs should evolve much faster than those of LMXBs [222], because the primary in MXRB is a massive early type Main Sequence star. Thus, LMXB SXTs should be more easily observed.

One more indication that SXTs belong to the class of LMXBs is their orbital period distribution. This is shown in Fig. 8.1a, where one can note that this distribution clusters around Log(P_{orb}) ≈ -0.4, where P_{orb} is expressed in days; this means that the orbital periods of SXTs have values which are mainly around 10 hours. A statistical tail due to GRO J1655-40 and V404 Cyg, whose secondaries are subgiants, is present. When one compares this distribution to the one made with all LMXBs (in Fig. 8.1b), the similarity between them is suddenly evident.

The distribution of SXTs with respect to the height z (in pc) over the Galactic Plane is shown in Fig. 8.2. Here the dashed and empty blocks represent Type I SXTs and Type II SXTs respectively. The corresponding probability distribution is instead shown in Fig. 8.3, where the continuous line refers to all SXTs, the long-dashed line to Type II SXTs and the short-dashed line to Type I SXTs. The scarcity of data points for Type I SXTs does not allow a comparison between the two distributions.

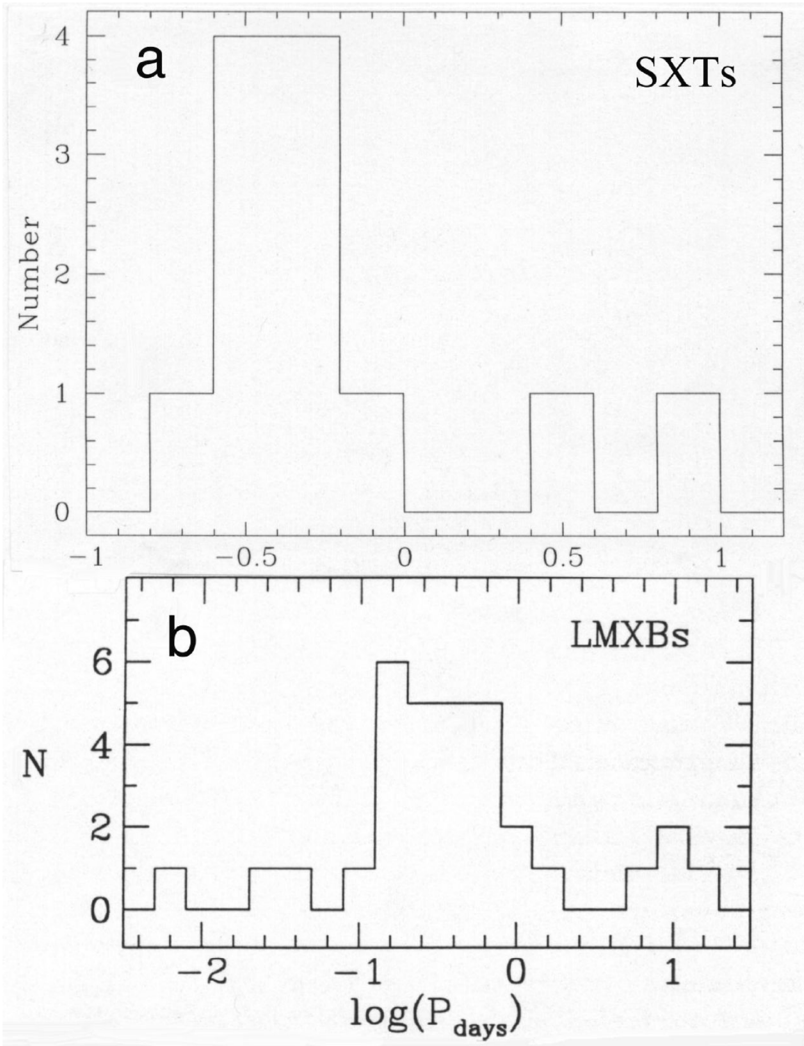

Fig. 8.1. a Orbital period distribution of SXTs. **b** Orbital period distribution of LMXBs (from [219]). Periods are expressed in days.

When z is not exactly known (see column 18 of Table 8.I) but is given in an interval of values, the central value has been taken. As one can see in Fig. 8.3, both Type I and Type II SXTs have a bimodal distribution along z with the primary maximum falling around 100 pc in both cases, while the secondary maximum is at a larger height for Type I SXTs (~500 pc, against ~350 pc in the case of Type II SXTs): this might be due to the larger supernova kick seen in systems harboring a NS [221]. It is therefore reasonable to suppose that a high-z SXT is more likely a Type I SXT; this statement should however be taken with some degree of caution since, as can be seen in column 18 of Table 8.I, some Type II SXTs are found at z > 400 pc. Moreover, it can also be noted in Fig. 8.3 that for z > 800 pc the probability distribution drops to zero. This is consistent with the z-distribution scale-height of Galactic LMXBs of ~900 pc, suggested by [219].

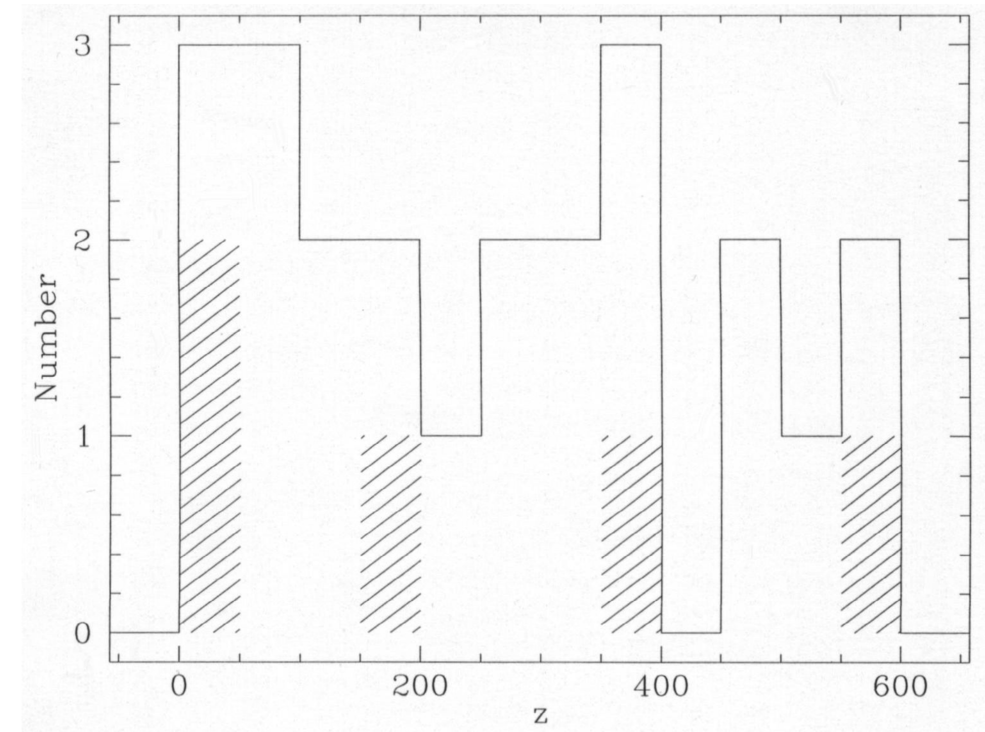

Fig. 8.2. Distribution of Galactic SXTs as a function of the height z over the Galactic Plane. Dashed blocks refer to Type I SXTs, empty blocks to Type II SXTs.

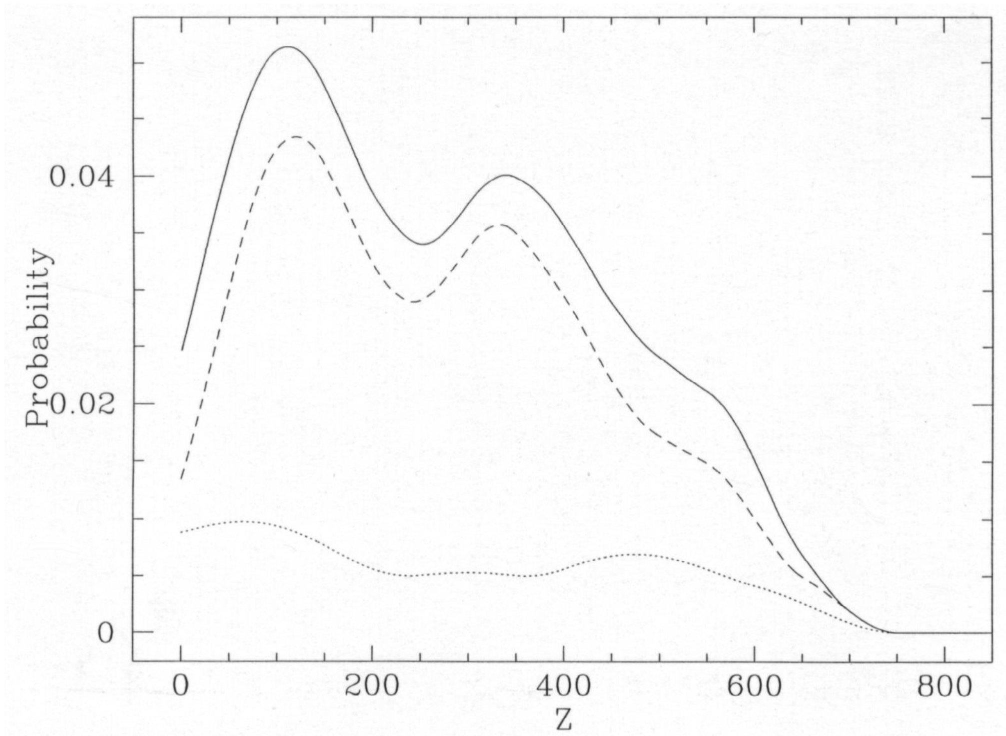

Fig. 8.3. Probability distribution versus z of Type I (short-dashed line), Type II (long-dashed line) and all (continuous line) SXTs.

As regards a possible correlation between z and the absolute magnitude M_V at maximum light, nothing remarkable is suggested by the plot in Fig. 8.4.

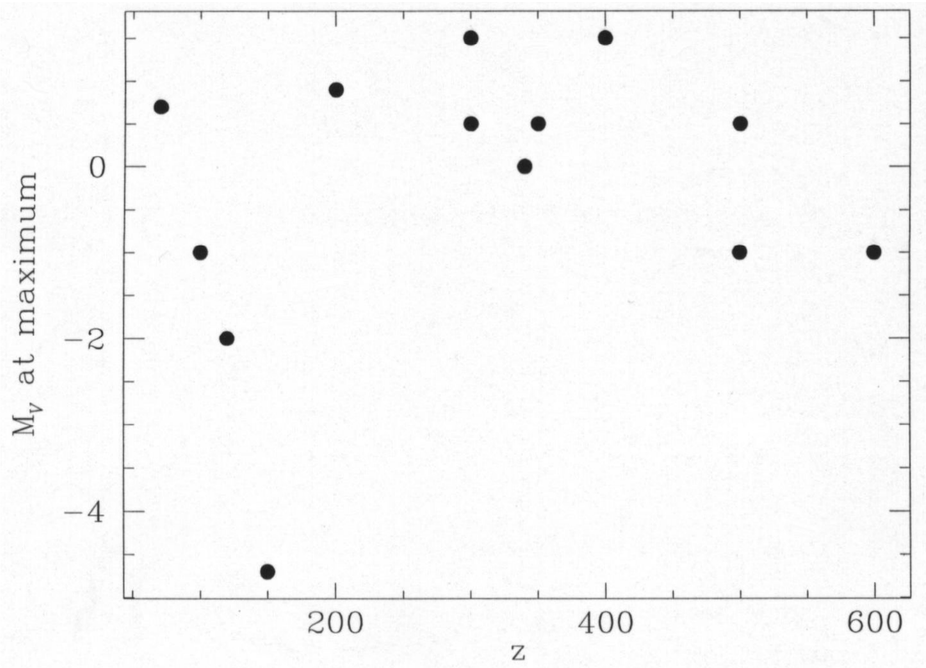

Fig. 8.4. Distribution of the absolute *V* magnitude of SXTs at maximum as a function of *z*. No correlation is clearly found between these two parameters.

The analysis of the recurrence times (column 6 of Table 8.I) of all the known outbursts of SXTs shows that in the last 30 years (that is, since the beginning of X-ray astronomy) 1.4 X-ray Nova events per year were observed; if one instead considers only the last outburst for each system, a slightly lower rate of ~1 event per year is obtained. One can also note that SXTs which recur over a period of about 10 years are 4 out of 5 (that is, 80%) among Type I SXTs, while only 3 out of 20 (i.e., 15%) display this chatacteristic among Type II SXTs. This might be possibly explained by the different X-ray illumination of the secondary during the quiescent phase: having the NSs a hot solid surface, the hard X-ray production in quiescence is higher than in BH SXTs (see column 32 of Table 8.I, where it can be seen that Type I SXTs have sistematically higher X-ray quiescent emission with respect to Type II SXTs) and the atmosphere of the secondary is more easily heated. This produces a higher quiescent $\dot{M}$ and favours a more rapid overcoming of the disk instability critical mass. On the contrary, in Type II SXTs the only hard X-ray source in the quiescent state is the inner part of the residual disk. This picture is supported by the model developed by [230].

8.3. X-RAY PROPERTIES OF SXTs

It has already been already widely discussed in Ch. 3 about the genesis, the behaviour and the evolution of X-ray emission in SXTs during the outburst. In this Section, therefore, the links and the correlations between what is related to the emission in this band and some important parameters of SXTs will be focused.

Let us start considering the X-ray emission at maximum, evaluated by means of Eq. (8.1) and of the values of peak fluxes and distances reported in columns 7 and 17 of Table 8.I, respectively. If one computes the logarithm of L_X at maximum, scaled with respect to the Eddington luminosity for 1 $M_\odot$, the correlation between this quantity and the logarithm of the ratio between the X-ray and optical luminosity at light peak (when both quantities are known; see column 12 of Table 8.I) can be studied. In this way, one obtains a sort of "color-magnitude" diagram over the optical and X-ray bands: this diagram is reported in Fig. 8.5.

The trend of this plot is not immediately clear; anyway, it seems that the lower is the X-ray luminosity at maximum, the lower is the L_X/L_{opt} ratio. The plot would also indicate that the optical luminosity of the system "saturates" under the effect of the X-ray irradiation; L_X may instead rise *ad libitum*, although in the limits imposed by the Eddington luminosity for the primary. In any case, there are some points (on the left of Fig. 8.5, near the 0 of the ordinates) which deviate from this behaviour.

In the previous Chapter it has been remarked the relation between the X-ray luminosity at maximum and the evolution of the FWHM of the H_α line in emission. This is once more a relation between optical and X-ray emissions. It has been shown that SXTs with maximum luminosities higher than ~10^{38} erg s^{-1} have accretion disks which expand as the outbursrt evolves, while SXTs with maximum luminosities below that limit show the opposite behaviour (Fig. 7.8). Anyway, due the poor statistics and the scanty data availability (this study was performed using the data of 5 Type II SXTs only), it is not possible either to state that this is a general behaviour for this class of objects, or say if Type I SXTs behave differently from Type II SXTs.

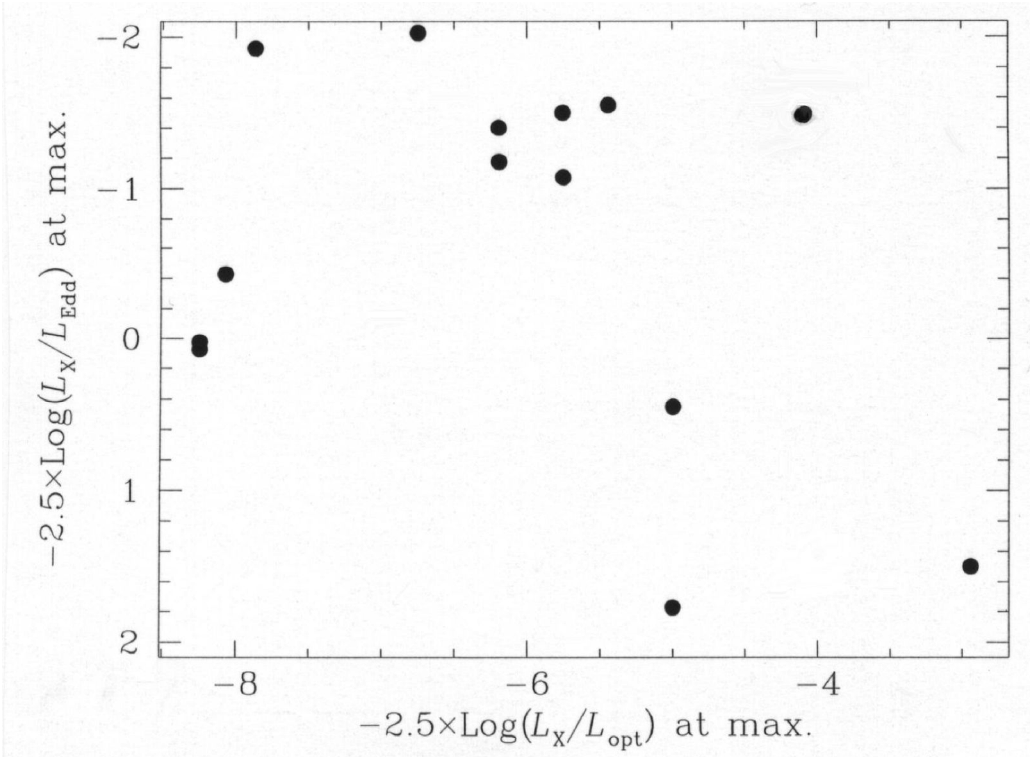

Fig. 8.5. "Color-magnitude" diagram of the logarithm of the L_X/L_{opt} ratio and the logarithm of the L_X/L_{Edd} ratio at light maximum in SXTs.

Let us now continue the analysis of the X-ray properties of SXTs by considering the decline phase. It was said in Sect. 2.3 that [141] showed that a linear relation, i.e. Eq. (3.10), exists between the *e*-folding decay time ($\tau_{1/e}$) of the X-ray light curve and the mass of the compact object. Actually, we see from column 23 of Table 8.I that 6 BHCs out of 7 have $\tau_{1/e}$ around, or greater than, 30 days (the only BHC for which this value is uncertain is GRO J1655-40 due to its complex X-ray light curve), while among Type I SXTs only V1333 Aql has $\tau_{1/e}$ around 30 days: all the remaining ones have instead $\tau_{1/e} \leq 10$ days. Concerning SXTs without spectroscopic primary mass determination, but possible BHCs, only one (MM Vel) has an X-ray *e*-folding decay time of about 10 days, while the 8 other SXTs for which $\tau_{1/e}$ is known have this parameter larger than 30 days. In 7 cases, the data are missing. If one plots the values of $\tau_{1/e}$ and M_1 for SXTs in which both are known, the trend shown in Fig. 8.6 is obtained.

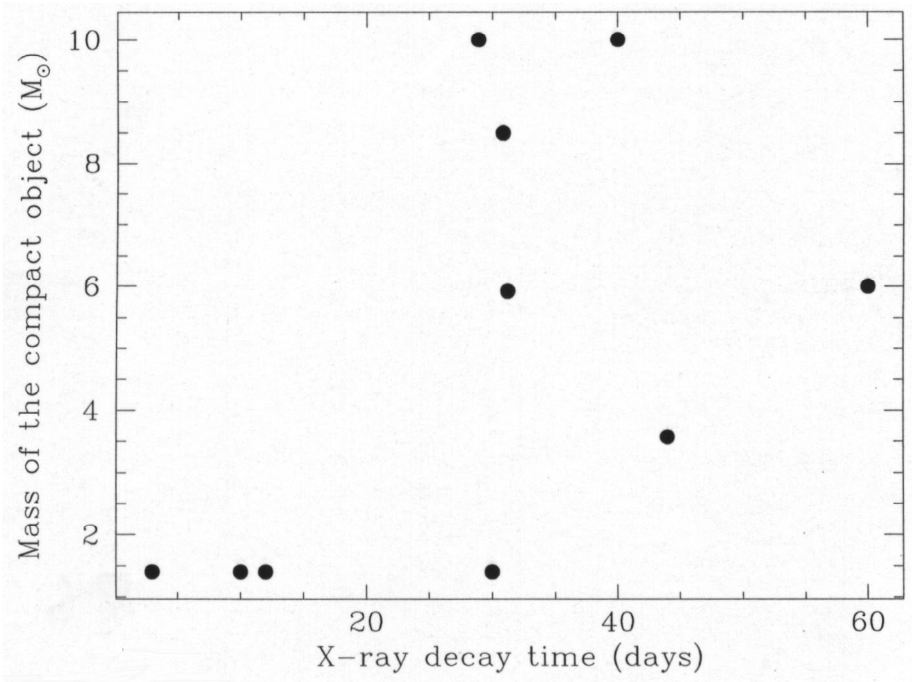

Fig. 8.6. Plot of primary masses of SXTs against X-ray light curve *e*-folding decay times for the cases in which both quantities are known. BHXNe fall in the upper right part of the Figure, while Type I SXTs are placed in the lower left part.

As it can be noticed, some correlation exists between the two quantities, even if some points (in particular that corresponding to Aql X-1) deviate from the general trend. It is however fairly evident that BHXNe are placed in the upper right part of Fig. 8.6, while Type I SXTs are in the opposite part, in the lower left corner of this Figure. One has however to remember that the scatter in Fig. 8.6 may also be due to the fact that $\tau_{1/e}$ is inversely dependent to the disk viscosity parameter α during outburst, which might assume different values in different systems.

The decline rate in X-ray appears to be univocally tied to that in the optical because of the considerations, already illustrated in Ch. 3, connected to the X-ray irradiation of the outer parts of the accretion disk and of the inner side of the secondary. This statement seems to find a confirmation in the plot reported in Fig. 8.7.

Particular attention deserves the relation between the moments of secondary X-ray maxima (column 25 of Table 8.I) and the duration of the orbital periods (column 33 of the same Table) in SXTs, which is plotted in Fig. 8.8. According to [223], the lower is the orbital period (i.e. the closer are the two stars), the closer is the secondary maximum to the primary one. Actually, Fig. 8.8 shows the the exactly opposite behaviour for the SXTs with Main Sequence or slightly evolved secondaries (for P_{orb} < 15 hours): the longer is the orbital period, and hence the distance between the stars, the earlier the secondary X-ray maximum occurs. Therefore it seems that, paradoxically, if the secondary maxima are due to a long-term response to the X-ray illumination [223], the closer is the system, the less the deep layers of the secondary star's atmosphere are heated and raised up. Thus, it may be suggested that an alternative mechanism (possibly involving the disk) is needed to explain the secondary X-ray maxima.

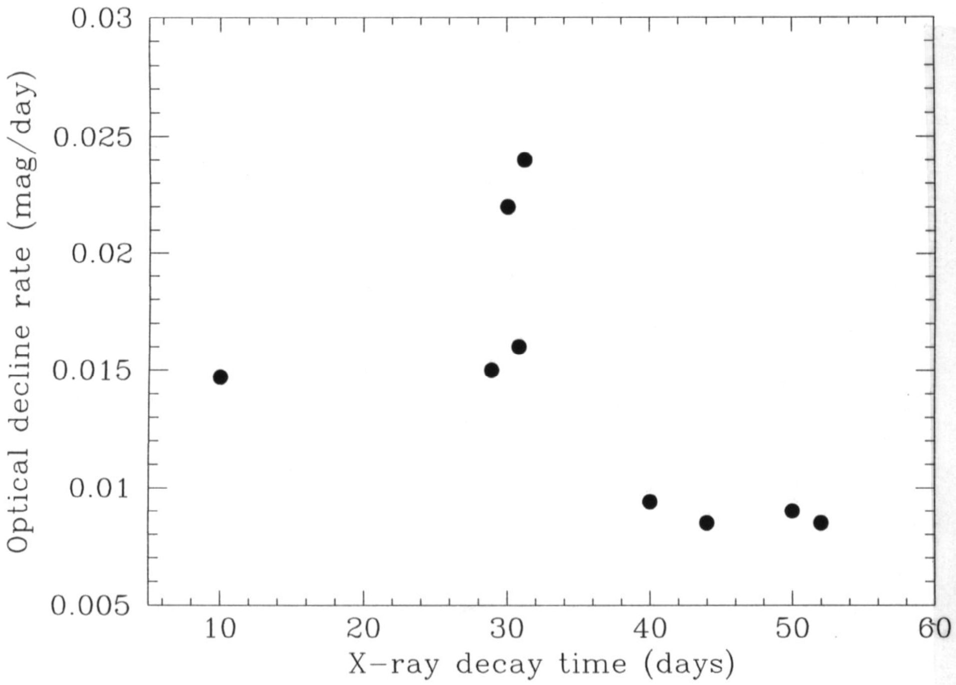

Fig. 8.7. Plot of the *e*-folding decay time of X-ray light curve against the decline rate of the optical light curve for SXTs in which both quantities are known. Longer X-ray decay times seem to correspond to slower optical decline rates.

The data corresponding to SXTs with subgiant companions, that is GRO J1655-40 and V404 Cyg, were not plotted in Fig. 8.8. Indeed, they are rather deviating from the trend described above; thus, such behaviour seems to hold only for SXTs with Main Sequence, or just slightly evolved, secondary. In fact, in the case of GRO J1655-40 there are no clear secondary maxima, but rather a series of repeated outbursts ([12]; see also Ch. 6).

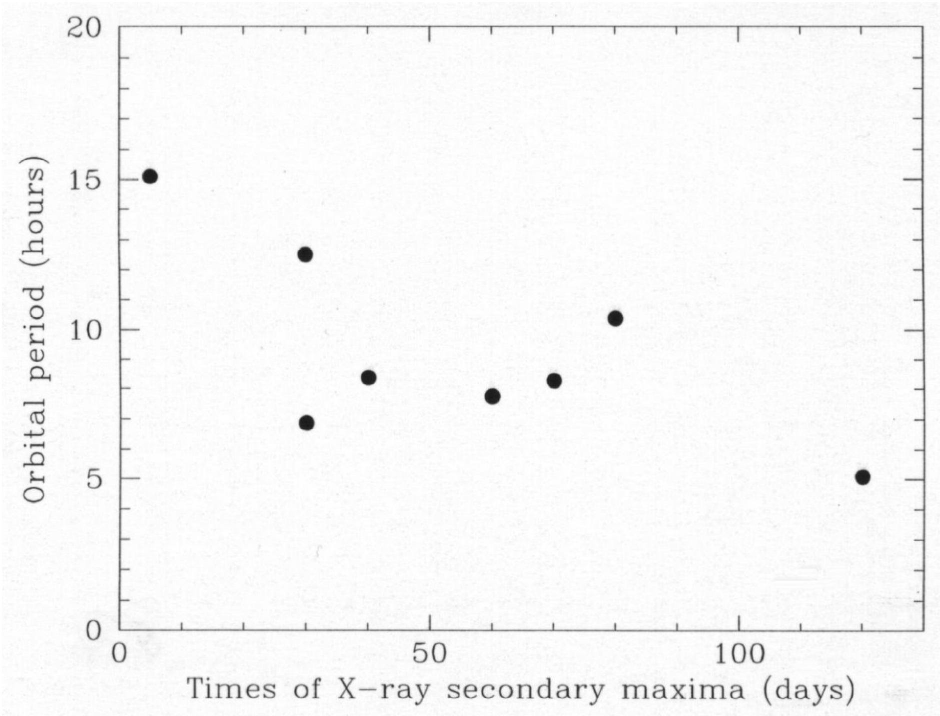

Fig. 8.8. Distribution of orbital periods as a function of the times of X-ray secondary maxima (expressed in days after the primary X-ray maximum) for SXTs with non-giant secondaries. Longer periods seem to imply secondary maxima closer to the X-ray peak.

As regards QPOs (column 10 of Table 8.I), we see that Type I SXTs have higher-frequency (~10^5 - 10^6 mHz) QPOs, while those of Type II SXTs have frequencies around 10 - 100 mHz. As QPOs are probably due to the interaction between the magnetic fields of the disk and of the central compact object [197], we could speculate that the presence of a rotating and weakly magnetized NS might produce high-frequency QPO, while a BH could not. QPOs in Type II SXTs might likely be rather related to the rotational frequency of the last stable orbit of the disk [231], hence the difference with the NS QPOs. Anyway, this point will deserve a deeper analysis in the future since it might become an important diagnostic to understand the nature of the compact object starting from the very first X-ray observations of outbursting SXTs.

On the contrary of what happens with Active Galactic Nuclei and with supermassive BHs (see e.g. [224] and references therein), the iron K_α X-ray emission does not seem a reliable tool for the classification of compact objects in SXTs. Indeed one can note that, out of the three systems which present this emission line in the X-ray spectrum (see column 46 of Table 8.I), one is a BHXN (V404 Cyg), one is a confirmed Type I SXT (QX Nor), and the third is a possible, but not confirmed, Type II SXT (IL Lup). It is thus clear that this diagnostic cannot be reliably used a index of the presence of a BH in these systems.

To this task, it appears instead more convincing the presence of the e^--e^+ annihilation line, as it is observed in several BHCs (see [190]) and in two confirmed BHXNe too (V518 Per and GU Mus; see column 46 in Table 8.I).

The X-ray luminosity at quiescence as a diagnostic to discriminate the nature of the compact object was already treated in the previous Section of this Chapter: here it will be briefly recalled that Type I SXTs are expected to have higher quiescent X-ray luminosity, likely due to the emission of the hot solid surface of the neutron star (see also [230]). This obviously cannot occur in quescent BHXNe as BHs do not have a surface, and the only sources of quiescent X-ray emission are the inner parts of the residual accretion disk.

8.4. OPTICAL PROPERTIES OF SXTs

In this Section the main properties of SXTs in the optical band during the outburst, the decline and the quiescence will be analyzed. One can begin, similarly to what was found in the previous Section and illustrated in Fig. 8.5, with a "color-magnitude" diagram at maximum light, with the *V* magnitude corrected for interstellar absorption plotted against the logarithm of the L_X/L_{opt} ratio at light peak. The diagram is shown in Fig. 8.9.

The trend, despite the presence of some deviant points, indicates a correlation between the two quantities, in the sense that the higher is the optical luminosity, the lower is the L_X/L_{opt} ratio. This behaviour might be explained by the fact that in SXTs the peak X-ray luminosity is the same within one order of magnitude for all of them; therefore, it is the optical luminosity at maximum, and then the response of the secondary and of the disk to the X-ray irradiation, that makes L_X/L_{opt} different in different cases. Reasonably, the optical magnitude at maximum depends on the size of the system, and thus of the secondary and of the disk. Indeed, the point in the upper right corner of Fig. 8.8 is referred to V404 Cyg, in which both the disk and the secondary must be wide, given the orbital period of 155.4 hours (= 6.48 days; it is the longest orbital period among SXTs) and the orbital semimajor axis of 34 $R_\odot$.

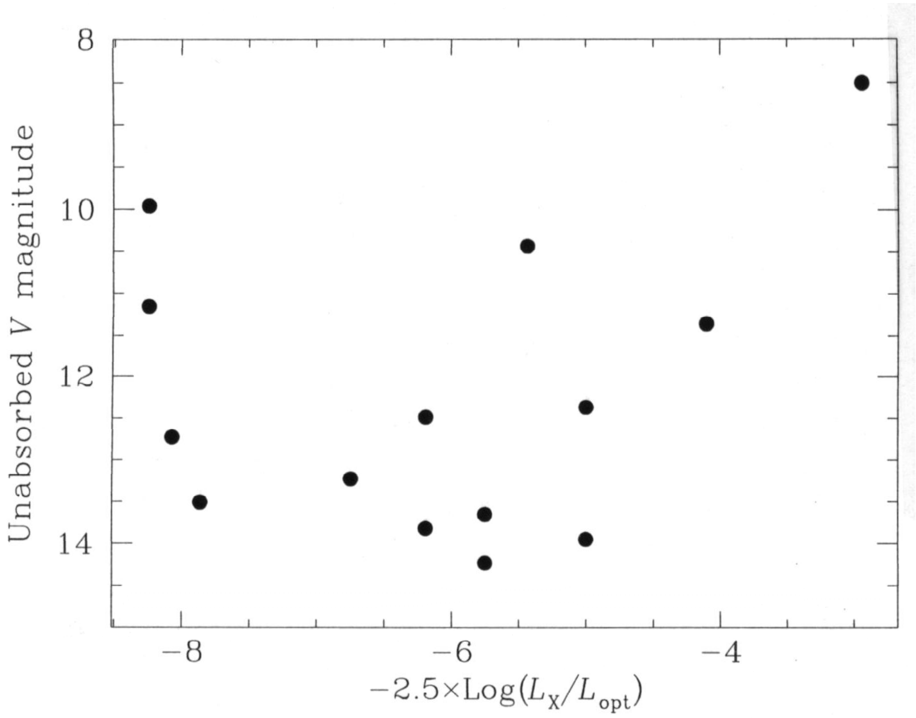

Fig. 8.9. "Color-magnitude" diagram for SXTs at maximum light between the unabsorbed *V* magnitude and the logarithm of the L_X/L_{opt} ratio.

This interpretation is further confirmed if one considers the relation, reported in Eq. (3.7), by [201]. In the hypothesis that for persistent LMXBs the optical luminosity depends on the X-ray illumination and on the size of the disk (thus on the size of the system itself, and finally on the length of the orbital period), the absolute magnitude M_V at maximum light will be a function of the parameter Σ defined by Eq. (3.8). The trend of M_V as a function of Σ for some persistent LMXBs (the values are taken from [201]) and for SXTs in outburst with known orbital (or superhump) period is represented in Fig. 8.10. In this Figure, SXTs are labeled with filled circles, while persistent LMXBs are indicated with filled triangles.

As one can see, outbursting SXTs are coherently placed on the best-fit line computed for persistent LMXBs by [201], and therefore show the same trend of persistent LMXBs: this implies that also in SXTs the peak optical light is due to the reprocessing of the X-ray radiation by the disk and possibly by the secondary; thus, also from this point of view, **SXTs at maximum light behave like persistent LMXBs**. This relation might then be used to determine the distance of SXTs with known orbital period, or vice versa to compute the orbital period if the distance is known.

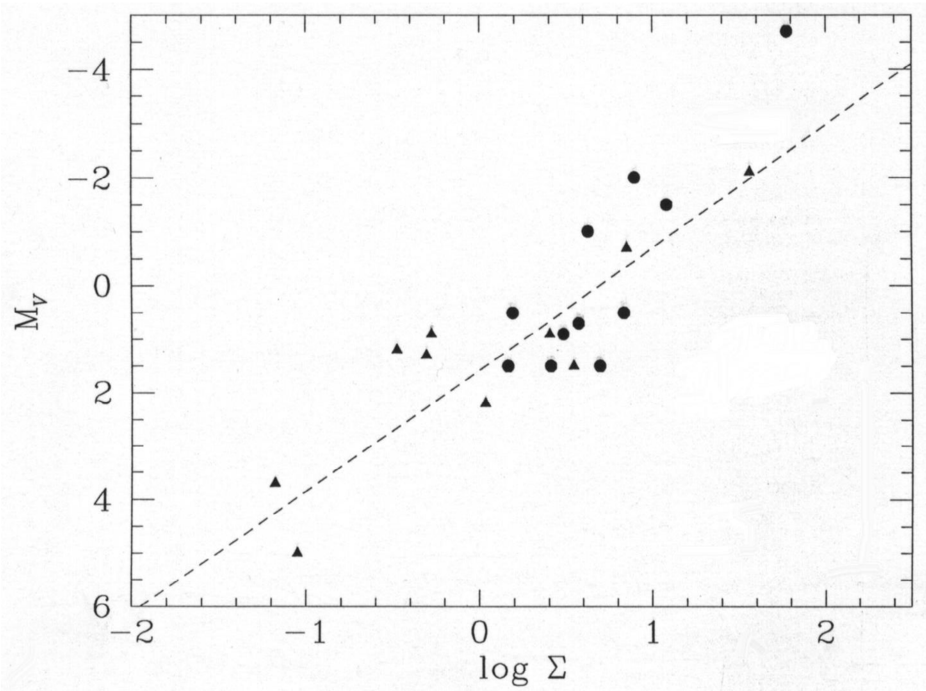

Fig. 8.10. Relation between the absolute *V* magnitude at light maximum and Log Σ for some SXTs (filled dots) and some persistent LMXBs (filled triangles). The line represents the linear least-squares fit by [201].

To this aim, we can try to estimate the orbital period of BW Cir, KY TrA and IL Lup using the data of Table 8.I. It is found a period of 100 - 150 hours for BW Cir (thus for this system the secondary should be a subgiant similar to the secondary of V404 Cyg), while for KY TrA and IL Lup orbital periods of ~10 hours and ~20 hours, respectively, are estimated; their secondaries should then be on the Main Sequence or slightly evolved stars.

Taking now into consideration the decline of the optical light curve, it must be remembered that, during this phase, SXTs may show superhumps: indeed, this kind of modulation has been detected in 5 cases, two of which (V2293 Oph and MM Vel) reported for the first time in papers originated in the framework of this Ph.D. Thesis (see Chs. 4 and 5, respectively). Moerover, all Type II SXTs and the majority of Type I SXTs seem to have a sufficiently low mass ratio q (see column 36 in Table 8.I) to allow the growth of an elliptic disk during the outburst, which is a mandatory condition for the development of superhumps, as we saw in Chs. 3, 4 and 5 of this Thesis and their bibliographies. According to [225], this kind of modulation should start to be detectable in SXTs after about 2 months after the X-ray peak, therefore around the secondary X-ray maximum.

If one however considers the results of Chs. 4 and 5, it follows that:

- in V2293 Oph, superhumps are already observed few weeks after the beginning of the outburst [133]. Moreover, the optical observational campaigns on the other SXTs with superhumps started few months after the light maximum [2, 37, 110, 134]: therefore, the detection of superhumps only after some weeks from the beginning of the outburst might well be a selection effect;
- in MM Vel a modulation is observed about one month before the secondary maximum [134]: thus, this secondary maximum may retrigger the disk instability already set up by the primary maximum;
- the superhump light curve in MM Vel (Fig. 5.7) shows the opposite symmetry with respect to 'classical' superhumps of SU UMas, while that in V2293 Oph gains back the 'correct' symmetry only after the subtraction of two underlying independent short-term modulations (Fig. 4.6). To this it should be added that also the superhump light curve of GU Mus [2] changes its shape as the optical decline proceeds. In this sense, if one observes an asymmetric modulation in the light curve of an outbursting SXT, this may be interpreted as a superhump even if it has a slow rise and a steep decline.

This group of characteristics in the light curve modulation (presence of superhumps already in the first stages of the outburst, change in the symmetry during the outburst evolution) is found in a peculiar subclass of SU UMas, the ER UMa stars. These systems (see Sect. 2.4) differ from ‘classical’ SU UMas [226, 227] because they have much shorter supercycles (40 - 50 days against 150 - 200 days in SU UMas) and superoutbursts which are much longer (20 days against ~10 days in SU UMas) and less bright (Δm ~ 3 mag against ~5 mag of ‘classical’ SU UMas). This behaviour seems to be due [226, 227] to the high $\dot{M}$ which characterizes ER UMa systems. A similar value, if not higher, for the mass transfer rate from the secondary is expected in SXTs during outburst because of the strong X-ray irradiation of the secondary: this would explain the similarities between these objects and the ER UMa-type DNe rather than the ‘classical’ SU UMas.

Let us now try to perform a statistical comparison among orbital periods, superhump periods and primary masses over the 3 systems for which these valus are known, that is V518 Per, QZ Vul and GU Mus. Clearly, given the rather small number of systems, this analysis must be considered only preliminar, with the hope to widen the SXT sample in the next future.

First of all, if one considers Eq. (2.7), one sees that it is always verified for the 3 SXTs mentioned above: this suggests that it might be a good indicator for the lower limit of the mass of the compact object even if the secondary is slightly evolved and if, together with the disk, is strongly irradiated by X-rays during the outburst.

Tabella 8.II. Values of the parameters ΔP (in percent) and η of the SXTs for which Eq. (2.8) is applicable.

SXT	ΔP (%)	η
V518 Per	0.0177	0.59
GU Mus	0.0154	0.47
QZ Vul	0.009	0.40

If we instead consider Eq. (2.8) one can note that, inserting the data of V518 Per, GU Mus and QZ Vul in this formula in order to evaluate the parameter η, it is found that (see Table 8.II) its value is around 0.5, thus slightly lower than that of DNe according to [228]. Since η depends on the quiescent disk radius, we speculate that the disks of quiescent SXTs are smaller than those of quiescent DNe. This might be due to the fact that the mass transfer rate from the secondary in SXTs at quiescence is very low, as the X-ray emission is almost undetected in this phase, especially in Type II SXTs; moreover, very little remains of the disk after the outburst.

As said before, this analysis should be obviously considered as preliminary due to the paucity of data. Therefore, it is premature to try to find a relation for SXTs similar to that found for SU UMas and illustrated by Eq. (2.9): the least one can say is that, in SXTs, superhump periods are 1-2 % longer than the correspondent orbital periods (see Table 8.II).

Considering now the optical properties during the late decline, it was seen in the previous Section that the optical decline rate is related to the decay time of the X-ray light curve. According to [35], the optical decline d*V*/d*t* (column 24 of Table 8.I) is tied to the orbital period by the relation

$$P_{\rm orb} = k\, e^{\alpha \frac{{\rm d}V}{{\rm d}t}} \tag{8.5}$$

where the orbital period is in hours, the optical decline rate in mag d^{-1}, $k = 3.9$ and $\alpha = 48.17$. This would mean (see [35]) that the closer are the components, the slower is the optical decline; therefore, the bulk of the optical emission would come from the X-ray heating of the secondary, and possibly of the outer parts of the disk. If we however integrate Fig. 6.14 of [35] by considering all the SXTs with known orbital period and optical decline rate, we obtain the trend reported in Fig. 8.11. The point correspondent to V822 Cen is highly deviant and falls well outside of the plot.

As one can see in Fig. 8.11, Eq. (8.5) seems to hold until Log ($P_{\rm orb}$) ~ 3, that is, until the secondary is a Main Sequence star. At longer periods, the trend is the opposite. This would mean that if the hypothesis by [35] is correct, subgiant secondaries cool down more slowly than Main Sequence stars, and that the cooling is slower when the star is larger. A least-squares fit analogous to that shown before, gives α = -168.2 and k = 696.6 for the right part of Fig. 8.11. Thus, summarizing, in SXTs with Main Sequence secondary the optical decline rate depends on the separation between the two components, while in the subgiant case the value of that parameter would be tied to the size of the secondary itself.

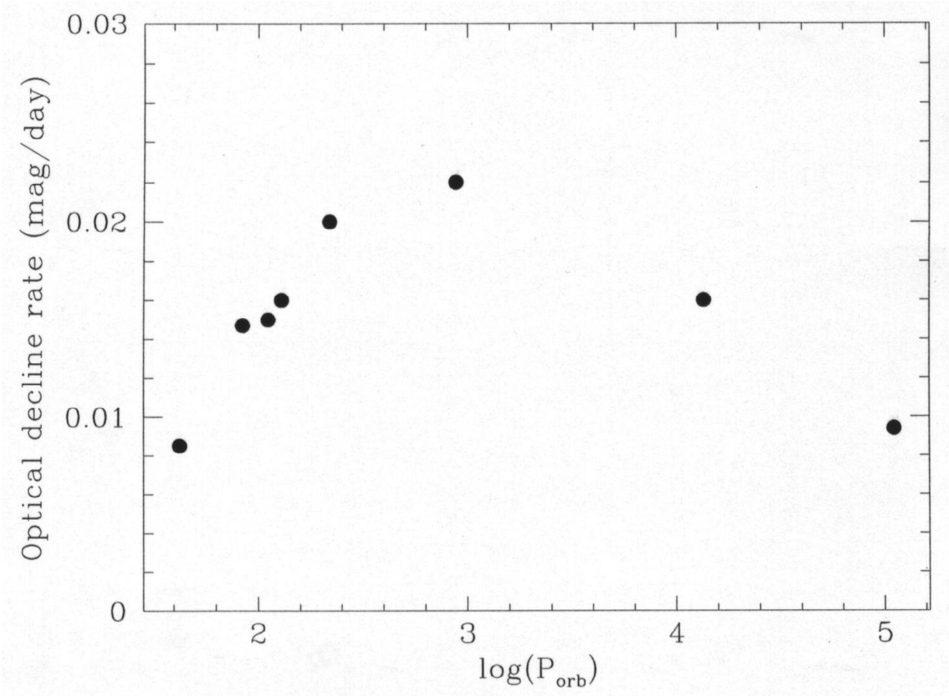

Fig. 8.11. Relation between the logarithm of the orbital period (expressed in hours) and the optical decline rate in SXTs for which both values are known. The point corresponding to V822 Cen falls outside the plot.

When the system has returned to quiescence, the spectrum of the secondary becomes detectable, as already said in Ch. 3. In this phase it might be possible to detect the presence of lithium in the atmosphere of the secondary. Indeed, in 5 cases the presence of Li λ6708 in absorption has been revealed (column 43 of Table 8.I). In the hypothesis [229] that this element is produced by X- and γ-ray spallation of CNO nuclei during the outburst and possibly also at quiescence, we can speculate that Type I SXTs, which seem to show shorter recurrence times and higher quiescent X-ray luminosities, have secondaries with higher Li abundances with respect to Type II SXTs. Indeed, from the values reported by [131] for SXTs in which the Li λ6708 has been detected, one can note that the Type II SXTs GU Mus, QZ Vul, V404 Cyg, V518 Per and V616 Mon have Li absorption lines with EW around 250 mÅ, while

Type I SXT V822 Cen has a Li line with EW = 480 mÅ [130]. So, the Li abundance in the secondaries of SXTs might be regarded as an interesting indicator of the nature of the compact object, since it seems from what illustrated above that the higher is the abundance of Li, the higher is the probability that the primary is a NS. At the very least, one can say that higher abundances of Li indicate shorter outburst recurrence times and/or higher quiescent X-ray luminosities.

8.5. CONCLUSIONS

The work developed during this three-year Ph.D. course and described in this Thesis allowed (or at least tried to allow) the increase of the knowledge of the characteristics of 4 X-ray Novae and the acquisition of new indications and hints on the properties and on the general features of SXTs as a class.

With the original data reported in this work (Chs. 4,5,6 and 7) it has indeed been possible to detect superhump modulations in V2293 Oph and in MM Vel, and to construct a simple geometric model for the description of this phenomenon; also, the orbital period of GRO J1655-40 has been confirmed and the outburst spectral evolution of this source has been analyzed; finally, the spectrophotometric decline of GU Mus has been described and an empyrical relation between the behaviour of the FWHM of the H_α emission line and the X-ray luminosity at maximum in some SXTs has been suggested.

Then, by means of an extensive biblioghraphic search, the main observational features of SXTs were gathered and correlated among one another. This allowed the detection or the confirmation of useful diagnostics to understand the nature of the collapsed object harboured in these sysrems well before the spectroscopic determination of its mass. These methods, besides that concerning the presence (or lack) of X-ray bursts or pulsations, are:

- the length of the superhump period and its comparison with the corresponding orbital period;

- the length of the *e*-folding decay time of the X-ray light curve;
- the recurrence time of the outbursts;
- the quiescent X-ray luminosity;
- the frequency of QPOs;
- the detection of the e^--e^+ annihilation line;
- the height *z* on the Galactic Plane;
- the abundance of Li on the secondary.

It has also been confirmed that SXTs belong to the class of LMXBs as both classes of object have similar Galactic distributions, similar orbital period distributions, and that the behaviour of the X-ray and optical emission during the outburst phase in SXTs is similar to that of persistent LMXBs.

Of course, a lot of work has still to be done in order to fully understand the mechanisms which trigger and rule the instability which generates the SXT outbursts, if MTI or ADI or both. In particular, it is needed to monitor the optical luminosity of quiescent SXTs, in order to understand the secular trend: it however seems [153] that it slowly increases with time. It should also be important to understand how the primary and secondary optical X-ray maxima occur in SXTs: this would help to understand their genesis; but this is possible only by means of an intense and simultaneous observational campaign in these two parts of the electromagnetic spectrum. Clearly, this is not an easy task, given the rapidity with which these phenomena occur.

Moreover, it is important to pursue the theoretical and observational study on analogies and differences between the optical behaviour during outburst in SXTs and in ER UMa-type DNe, since it seems that there exists some affinity between these two classes of objects, particularly for what concerns the superhump modulation. It is also importat to try to increase the statistics concerning the relations found in this work inside the class of SXTs, with particular attention to that between the X-ray luminosity at maximum and the FWHM of H_α emission line, in order to verify whether or not a difference in the behaviour of Type I and Type II SXTs exists.

All this will however be possible only thanks to new observations of SXTs during the outburst phase. Quiescent observations, instead, will give the opportunity to determine orbital periods and primary mass functions for those objects in which these quantities are still unknown (see Table 8.I).

As one can see from this last Section, even if in the last years the knowledge on SXTs increased very rapidly, a lot of 'dark places' remain, which need new and deeper observations or a stronger effort in the theoretical interpretation. The field is however of fundamental interest, as it allows the observational and theoretical study of the binary systems in which most likely are hidden the last taboos of modern astronomy: black holes.

REFERENCES OF CHAPTER 8

[1] Asai K., Dotani T., Mitsuda K. et al., 1996, PASJ, 48, 257
[2] Bailyn C.D., 1992, ApJ, 391, 298
[3] Bailyn C.D., Orosz J.A., 1995, ApJ, 440, L73
[4] Bailyn C.D., Orosz J.A., Girard T.M. et al., 1995, Nat, 374, 701
[5] Bailyn C.D., Orosz J.A., McClintock J.E., Remillard R.A., 1995, Nat, 378, 157
[6] Ball L., Kesteven M.J., Campbell-Wilson D., Turtle A.J., Hjellming R.M., 1995, MNRAS, 273, 722
[7] Barret D., Roques J.P., Mandrou P. et al., 1992, ApJ, 392, L19
[8] Barret D., Bouchet L., Mandrou P. et al., 1992, ApJ, 394, 615
[9] Barret D., Motch C., Pietsch W., Voges W., 1995, A&A, 296, 459
[10] Bartolini C., Guarnieri A., Piccioni A., Beskin G.M., Neizvestny S.I., 1994, ApJS, 92, 455
[11] Berger M., van der Klis M., van Paradijs J. et al., 1996, ApJ, 469, L13
[12] Bianchini A., Della Valle M., Masetti N., Margoni R., 1997, A&A, 321, 477 *(Chapter 6 of this Thesis)*
[13] Blair W.P., Raymond J.C., Dupree A.K. et al., 1984, ApJ, 278, 270
[14] Boley F., Wolfson R., Bradt H.V. et al., 1976, ApJ, 203, L13
[15] Borisov N.V., Bochkarev N.G., Gladyshev S.A. et al., 1989, X-ray nova GS 2000+25 = Nova Vul 1988: X-ray and optical light curves, spectra and model. In: Hunt J., Battrick B. (eds.) Proc. 23rd ESLAB Symposium on Two Topics in X-Ray Astronomy (ESA SP-296). ESA Publication Division, ESTEC, Noordwijk, vol. 1, p. 305
[16] Borozdin K.N., Alexandrovich N.L., 1994, IAU Circ. 6083
[17] Borozdin K.N., Alexandrovich N.L., Sunyaev R.A., 1995, IAU Circ. 6141
[18] Borozdin K.N., Alexandrovich N.L., Aref'ev V.A., Sunyaev R.A., Skinner G.K., 1995, Astron. Lett., 21, 212
[19] Bouchacourt P., Chambron G., Niel M. et al., 1984, ApJ, 285, L67
[20] Brandt W.N., Podsiadlowski P., Sigurdsson S., 1995, MNRAS, 277, L35
[21] Branduardi G., Ives J.C., Sanford P.W., Brinkman A.C., Maraschi L., 1976, MNRAS, 175, 47P
[22] Callanan P.J., Garcia M.R., McClintock J.E. et al., 1995, ApJ, 441, 786
[23] Callanan P.J., Garcia M.R., McClintock J.E. et al., 1996, ApJ, 461, 351
[24] Callanan P.J., Garcia M.R., Filippenko A.V., McLean I., Teplitz H., 1996, ApJ, 470, L57
[25] Canizares C.R., McClintock J.E., Grindlay J.E., 1980, ApJ, 236, L55
[26] Casares J., Charles P.A., 1994, MNRAS, 271, L5
[27] Casares J., Charles P.A., Jones D.H.P., Rutten R.H.G., Callanan P.J., 1991, MNRAS, 250, 712
[28] Casares J., Charles P.A., Naylor T., 1992, Nat, 355, 614
[29] Casares J., Charles P.A., Naylor T., Pavlenko E.P., 1993, MNRAS, 265, 834
[30] Casares J., Martin A.C., Charles P.A. et al., 1995, MNRAS, 276, L35
[31] Casares J., Charles P.A., Marsh T.R., 1995, MNRAS, 277, L45
[32] Casares J., Martín E.L., Charles P.A., Molaro P., Rebolo R., 1996, NewA, 1, 299
[33] Castro-Tirado A.J., Pavlenko E.P., Shlyapnikov A.A. et al., 1992, IAU Circ. 5588
[34] Castro-Tirado A.J., Pavlenko E.P., Shlyapnikov A.A. et al., 1993, A&A, 276, L37
[35] Castro-Tirado A.J., 1995, Ph.D. Thesis, University of Copenhagen
[36] Charles P.A., Thorstensen J.R., Bowyer S. et al., 1980, ApJ, 237, 154
[37] Charles P.A., Kidger M.R., Pavlenko E.P., Prokofieva V.V., Callanan P.J., 1991, MNRAS, 249, 567
[38] Charles P.A., Southwell K.A., O'Donoghue D., 1996, IAU Circ. 6305
[39] Cheng F.H., Horne K., Panagia N. et al., 1992, ApJ, 397, 644
[40] Chevalier C., 1989, Unusual counterparts of Soft X-ray Transients 4U1543-47 and 4U2129+47 in quiescence: interlopes or third stars?. In: Hunt J., Battrick B. (eds.) Proc. 23rd ESLAB Symposium on Two Topics in X-Ray Astronomy (ESA SP-296). ESA Publication Division, ESTEC, Noordwijk, vol. 1, p. 341
[41] Chevalier C., Ilovaisky S.A., 1990, A&A, 238, 163
[42] Chevalier C., Ilovaisky S.A., 1991, A&A, 251, L11
[43] Chevalier C., Ilovaisky S.A., 1993, A&A, 269, 301
[44] Chevalier C., Ilovaisky S.A., 1995, A&A, 297, 103
[45] Chevalier C., Ilovaisky S.A., 1996, A&A, 312, 105
[46] Chevalier C., Ilovaisky S.A., van Paradijs J., Pedersen H., van der Klis M., 1989, A&A, 210, 114

[47] Chiappetti L., White N.E., Kahn S.M., Shafer R., 1985, Space Sci. Rev., 40, 207
[48] Clark C., Remillard R.A., Woo J., 1996, IAU Circ. 6282
[49] Cominsky L., Jones C., Forman W., Tananbaum H.D., 1978, ApJ, 224, 46
[50] Conner J.P., Evans W.D., Belian R.D., 1969, ApJ, 157, L157
[51] Cooke B.A., Levine A.M., Lang F.M., Primini F.A., Lewin W.H.G., 1984, ApJ, 285, 258
[52] Cowley A.P., Hutchings J.B., Crampton D., 1988, ApJ, 333, 906
[53] Cowley A.P., Schmidtke P.C., Crampton D., Hutchings J.B., Bolte M., ApJ, 1991, 373, 228
[54] Czerny M., Czerny B., Grindlay J.E., 1987, ApJ, 312, 122
[55] Davies R.D., Walsh D., Browne I.W.A., Edwards M.R., Noble R.G., 1976, Nat, 261, 476
[56] Davis R.J., Edwards M.R., Morison I., Spencer R.E., 1975, Nat, 257, 659
[57] Davison P., Burnell J. Ives J.C., 1976, IAU Circ. 2925
[58] Della Valle M., 1992, ESO Messenger, 67, 35
[59] Della Valle M., Benetti S., 1993, IAU Circ. 5890
[60] Della Valle M., Jarvis B.J., West R.M., 1991, Nat, 353, 50
[61] Della Valle M., Mirabel I.F., Rodriguez L.F., 1994, A&A, 290, 803
[62] Della Valle M., Benetti S., Cappellaro E., Wheeler J.C., 1997, A&A, 318, 179
[63] Della Valle M., Masetti N., Bianchini A., 1998, A&A, 329, 606 *(Chapter 7 of this Thesis)*
[64] Doxsey R., Jernigan G., Hearn D. et al., 1976, ApJ, 203, L9
[65] Durouchoux P., Smith I.A., Hurley K. et al., 1996, IAU Circ. 6383
[66] Eachus L.J., Wright E.J., Liller W., 1976, ApJ, 203, L17
[67] Ebisawa K., Mitsuda K., Hanawa T., 1991, ApJ, 367, 213
[68] Ebisawa K., Ogawa M., Aoki T. et al., 1994, PASJ, 46, 375
[69] Elvis M., Page C.G., Pounds K.A., Ricketts M.J., Turner M.J.L., 1975, Nat, 257, 656
[70] Eyles C.J., Skinner G.K., Willmore A.P., Rosenberg F.D., 1975, Nat, 257, 291
[71] Fabbiano G. Gursky H., Schwartz D.A., Schwartz J., 1978, ApJ, 221, L49
[72] Filippenko A.V., Matheson T., Ho L.C., 1995, ApJ, 455, 614
[73] Filippenko A.V., Matheson T., Barth A.J., 1995, ApJ, 455, L139
[74] Forman W., Jones C., Tananbaum H.D., 1976, ApJ, 207, L25
[75] Forman W., Jones C., Cominsky L. et al., 1978, ApJS, 38, 357
[76] Francey R.J., 1971, Nat. Phys. Sci., 229, 229
[77] Goldwurm A., Ballet J., Cordier B. et al., 1992, ApJ, 389, L79
[78] Goranskij V.P., Karitskaya E.A., Kurochkin N.E., Trunkovskij E.M., 1996, Astron. Lett., 22, 371
[79] Gotthelf E., Patterson J., Stover R.J., 1991, ApJ, 374, 340
[80] Gotthelf E., Halpern J.P., Patterson J., Rich R.M., 1992, AJ, 103, 219
[81] Grebenev S.A., Sunyaev R.A., Pavlinskij M.N., 1992, SvA Lett., 18, 5
[82] Greiner J., 1994, IAU Circ. 6078
[83] Greiner J., Dennerl K., Predehl P., 1996, A&A, 314, L21
[84] Griffiths R.E., Bradt H.V., Doxsey R. et al., 1978, ApJ, 221, L63
[85] Grindlay J.E., Liller W., 1978, ApJ, 220, L127
[86] Han X.H., Hjellming R.M., 1992, ApJ, 400, 304
[87] Harlaftis E.T., Horne K., Filippenko A.V., 1996, PASP, 108, 762
[88] Harmon B.A., Wilson R.B., Finger M.H. et al., 1992, IAU Circ. 5504
[89] Harmon B.A., Fishman G.J., Paciesas W.S., Zhang S.N., 1993, IAU Circ. 5900
[90] Harmon B.A., Wilson C.A., Zhang S.N. et al., 1995, Nat, 374, 703
[91] Hasinger G., van der Klis M., 1989, A&A, 225, 79
[92] Hertz P., Grindlay J.E., 1983, ApJ, 275, 105
[93] Hjellming R.M., Rupen M.P., 1995, Nat, 375, 464
[94] Hjellming R.M., Calovini T.A., Han X.H., Còrdova F. A., 1988, ApJ, 35, L75
[95] Hjellming R.M., Han X.H., Roussel-Dupré D., 1990, IAU Circ. 5112
[96] Hjellming R.M., Rupen M.P., Martì I., Mirabel I.F., Rodriguez L.F., 1996, IAU Circ. 6383
[97] Ilovaisky S.A., Chevalier C., 1996, IAU Circ. 6416
[98] Ilovaisky S.A., Pedersen H., van der Klis M., 1987, IAU Circ. 4362
[99] Jernigan J.G., Apparao K.M.V., Bradt H.V. et al., 1978, Nat, 272, 701
[100] Johnston H.M., Verbunt F., Hasinger G., 1995, A&A, 298, L21
[101] Jones C., 1977, ApJ, 214, 856
[102] Jones C., Forman W., Tananbaum H.D., Turner M.J.L, 1976, ApJ, 210, L9
[103] Jones D., Carter D., 1989, IAU Circ. 4794
[104] Kaluzienski L.J., Holt S.S., 1977, IAU Circ. 3099
[105] Kaluzienski L.J., Holt S.S., Boldt E.A. et al., 1975, ApJ, 201, L121

[106] Kaluzienski L.J., Holt S.S., Boldt E.A., Serlemitsos P.J., 1977, ApJ, 212, 203
[107] Kaluzienski L.J., Holt S.S., Boldt E.A., Serlemitsos P.J., 1977, Nat, 265, 606
[108] Kaluzienski L.J., Holt S.S., Swank J.H., 1980, ApJ, 241, 779
[109] Karitskaya E.A., Goranskij V.P., 1995, IAU Circ. 6174
[110] Kato T., Mineshige S., Hirata R., 1995, PASJ, 47, 31
[111] Kellogg E., Gursky H., Murray S., Tananbaum H.D., Giacconi R., 1971, ApJ, 169, L99
[112] Kitamoto S., Tsunemi H., Miyamoto S. et al., 1989, Nat, 342, 518
[113] Kitamoto S., Tsunemi H., Pedersen H., Ilovaisky S.A., van der Klis M., 1990, ApJ, 361, 590
[114] Kitamoto S., Tsunemi H., Miyamoto S., Hayashida K., 1992, ApJ, 394, 609
[115] Kitamoto S., Tsunemi H., Miyamoto S., Roussel-Dupré D., 1993, ApJ, 403, 315
[116] Koyama K., Inoue H., Makishima K. et al., ApJ, 1981, 247, L27
[117] Kudryavtsev M.I., Svertilov S.I., Bogomolov V.V., 1995, Astron. Lett., 21, 224
[118] Lapshov I.Y., Dremin V.V., Sunyaev R.A. et al., 1992, SvA Lett., 18, 1
[119] Lapshov I.Y., Sazonov S.Y., Sunyaev R.A. et al., 1994, Astron. Lett., 20, 205
[120] Levine A.M., Bradt H., Chakrabarty D. et al., 1996, IAU Circ. 6390
[121] Li F.K., Sprott G.F., Clark G.W., 1976, ApJ, 203, 187
[122] Lochner J.C., Roussel-Dupré D., 1994, ApJ, 435, 840
[123] Long K.S., Kestenbaum H.L., 1978, ApJ, 226, 271
[124] Lyutyi V.M., Shugarov S.Y., 1979, SvA Lett., 5, 206
[125] Maeda Y., Koyama K., Sakano M., Takeshima T., Yamauchi S., 1996, PASJ, 48, 417
[126] Marsh T.R., Robinson E.L., Wood J.H., 1994, MNRAS, 266, 137
[127] Marshall F.E., Angelini L., 1996, IAU Circ. 6331
[128] Martin A.C., Casares J., Charles P.A., van der Hooft F., van Paradijs J., 1995, MNRAS, 274, L46
[129] Martín E.L., Rebolo R., Casares J., Charles P.A., 1992, Nat, 358, 129
[130] Martín E.L., Rebolo R., Casares J., Charles P.A., 1994, ApJ, 435, 791
[131] Martín E.L., Casares J., Molaro P., Rebolo R., Charles P.A., 1996, NewA, 1, 197
[132] Martins D.H., Harvel C.A., Miller D.H., 1980, AJ, 85, 521
[133] Masetti N., Bianchini A., Bonibaker J., Della Valle M., Vio R., 1996, A&A, 314, 123 *(Chapter 4 of this Thesis)*
[134] Masetti N., Bianchini A., Della Valle M., 1997, A&A, 317, 769 *(Chapter 5 of this Thesis)*
[135] Matilsky T.A., Giacconi R., Gursky H., Kellogg E.M., Tananbaum H.D., 1972, ApJ, 174, L53
[136] Matilsky T.A., Bradt H.V., Buff J. et al., 1976, ApJ, 210, L127
[137] Matsuoka M., Inoue H., Koyama K. et al., 1980, ApJ, 240, L137
[138] McClintock J.E., Remillard R.A., 1986, ApJ, 308, 110
[139] McClintock J.E., Remillard R.A., 1990, ApJ, 350, 386
[140] McClintock J.E., Horne K., Remillard R.A., 1995, ApJ, 442, 358
[141] Mineshige S., Yamasaki T., Ishizaka C., 1993, PASJ, 45, 707
[142] Mirabel I.F., Marti J., Duc P.A., Rodriguez L.F., 1996, IAU Circ. 6427
[143] Miyamoto S., Kitamoto S., Iga S., Negoro H., Terada K., 1992, ApJ, 391, L21
[144] Morgan E.H., Smith D.A., 1996, IAU Circ. 6437
[145] Murakami T., Inoue H., Makishima K., Hoshi R., 1987, PASJ, 39, 879
[146] Murdin P., Griffiths R.E., Pounds K.A., Watson M.G., Longmore A.J., 1977, MNRAS, 178, 27P
[147] Murdin P., Allen D.A., Morton D.C., Whelan J.A.J., Thomas R.M., 1980, MNRAS, 192, 709
[148] Oke J.B., 1977, ApJ, 217, 181
[149] Oke J.B., Greenstein J.L., 1977, ApJ, 211, 872
[150] Oosterbroek T., van der Klis M, Vaughan B. et al., 1996, A&A, 309, 781
[151] Orosz J.A., Bailyn C.D., 1995, ApJ, 446, L59
[152] Orosz J.A., Bailyn C.D., Remillard R.A., McClintock J.E., Foltz C.B., 1994, ApJ, 436, 848
[153] Orosz J.A., Bailyn C.D., McClintock J.E., Remillard R.A., 1996, ApJ, 468, 380
[154] Paciesas W.S., Briggs M.S., Harmon B.A., Wilson R.B., Finger M.H., 1992, IAU Circ. 5580
[155] Paciesas W.S., Harmon B.A., Rubin B.C. et al., 1995. In: Signore M., Salati P., Vedrenne G. (eds.) The Gamma-Ray Sky with Compton GRO and SIGMA. Kluwer Acad. Publ., Dordrecht, p. 221
[156] Parmar A.N., Stella L., White N.E., 1986, ApJ, 304, 664
[157] Parmar A.N., Angelini L., Roche P., White N.E., 1993, A&A, 279, 179
[158] Parmar A.N., Angelini L., White N.E., 1995, ApJ, 452, L129
[159] Pavlenko E.P., Prokofieva V.V., Dolgushin A.I., 1989, SvA Lett., 15, 262

[160] Pavlenko E.P., Martin A.C., Casares J., Charles P.A., Ketsaris N.A., 1996, MNRAS, 281, 1094
[161] Pedersen H., 1983, ESO Messenger, 34, 21
[162] Penninx W., Damen E., Tan J., Lewin W.H.G., van Paradijs J., 1989, A&A, 208, 146
[163] Predehl P., Schmitt J.H.M.M., 1995, A&A, 293, 889
[164] Remillard R.A., McClintock J.E., Bailyn C.D., 1992, ApJ, 399, L145
[165] Remillard R.A., Orosz J.A., McClintock J.E., Bailyn C.D., 1996, ApJ, 459, 226
[166] Richter G.A., 1989, IBVS No. 3362
[167] Ricketts M.J., Pounds K.A., Turner M.J.L., 1975, Nat, 257, 657
[168] Roques J.P., Bouchet L., Jourdain E. et al., 1994, ApJS, 92, 451
[169] Sanwal D., Robinson E.L., Zhang E. et al., 1996, ApJ, 460, 437
[170] Schoelkopf R.J., Kelley R.L., 1991, ApJ, 375, 696
[171] Shahbaz T., Naylor T., Charles P.A., 1994, MNRAS, 268, 756
[172] Shahbaz T., Ringwald F.A., Bunn J.C. et al., 1994, MNRAS, 271, L10
[173] Shahbaz T., Bandyopadhyay R., Charles P.A., Naylor T., 1996, MNRAS, 282, 977
[174] Shahbaz T., van der Hooft F., Charles P.A., Casares J., van Paradijs J., 1996, MNRAS, 282, L47
[175] Shrader C.R., Wagner R.M., Hjellming R.M., Han X.H., Starrfield S.G., 1994, ApJ, 434, 698
[176] Shvartsman V.F., Beskin G.M., Mitronova S.N., Neizvestny S.I., Plakhotnichenko V.L., 1989, SvA Lett., 15, 252
[177] Skinner G.K., Foster A.J., Willmore A.P., Eyles C.J., 1990, MNRAS, 243, 72
[178] Stella L., Campana S., Colpi M., Mereghetti S., Tavani M., 1994, Mem. Soc. Astron. Ital., 65, 311
[179] Sunyaev R.A., 1989, IAU Circ. 4839
[180] Sunyaev R.A., Lapshov I.Y., Grebenev S.A. et al., 1988, SvA Lett., 14, 327
[181] Sunyaev R.A., Gilfanov M., Churazov E. et al., 1989, A new transient X-ray source near GX 1+4. In: Hunt J., Battrick B. (eds.) Proc. 23rd ESLAB Symposium on Two Topics in X-Ray Astronomy (ESA SP-296). ESA Publication Division, ESTEC, Noordwijk, vol. 1, p. 641
[182] Sunyaev R.A., Gilfanov M., Churazov E. et al., 1990, SvA Lett., 16, 59
[183] Sunyaev R.A., Kaniovskij A.S., Efremov V.V. et al., 1991, SvA Lett., 17, 123
[184] Sunyaev R.A., Churazov E., Gilfanov M. et al., 1992, ApJ, 389, L75
[185] Sunyaev R.A., Kaniovskij A.S., Borozdin K.N. et al., 1993, A&A, 280, L1
[186] Sunyaev R.A., Borozdin K.N., Alexandrovich N.L. et al., 1994, Astron. Lett., 20, 777
[187] Suzuki K., Matsuoka M., Inoue H. et al., 1984, PASJ, 36, 761
[188] Szkody P., Margon B., 1989, IAU Circ. 4794
[189] Tanaka Y., 1989, Black holes in X-ray binaries: X-ray properties of the galactic black hole candidates. In: Hunt J., Battrick B. (eds.) Proc. 23rd ESLAB Symposium on Two Topics in X-Ray Astronomy (ESA SP-296). ESA Publication Division, ESTEC, Noordwijk, vol. 1, p. 3
[190] Tanaka Y., Lewin W.H.G., 1995, Black-hole binaries. In: Lewin W.H.G., van Paradijs J., van den Heuvel E.P.J. (eds.) X-Ray Binaries. Cambridge Univ. Press, p. 126
[191] Thorstensen J.R., Charles P.A., Bowyer S., 1978, ApJ, 220, L131
[192] Tingay S.J., Jauncey D.L., Preston R.A. et al., 1995, 374, 141
[193] Trudolyubov S.P., Gilfanov M.R., Churazov E.M. et al., 1996, Astron. Lett., 22, 664
[194] Tsunemi H., Kitamoto S., Okamura S., Roussel-Dupré D., 1989, ApJ, 337, L81
[195] Udalski A., Kaluzny J., 1991, PASP, 103, 198
[196] van der Hooft F., Kouvelioutou C., van Paradijs J. et al., 1996, ApJ, 458, L75
[197] van der Klis M., 1995, Rapid Variability in X-ray Binaries - Toward a Unified Description. In: Alpar M.A., Kizioglu Ü., van Paradijs J. (eds.) The Lives of the Neutron Stars. Kluwer Acad. Publ., Dordrecht, p. 301
[198] van der Woerd H., White N.E., Kahn S.M., 1989, ApJ, 344, 320
[199] van Dijk R., Bennett K., Collmar W. et al., 1995, A&A, 296, L33
[200] van Paradijs J., 1995, A catalogue of X-ray binaries. In: Lewin W.H.G., van Paradijs J., van den Heuvel E.P.J. (eds.) X-ray Binaries. Cambridge Univ. Press, p. 536
[201] van Paradijs J., McClintock J.E., 1994, A&A, 290, 133
[202] van Paradijs J., Verbunt F., 1984. In: Woosley S. (ed.) High Energy Transients in Astrophysics, AIP Conf. Proc. 115. AIP, New York, p. 49
[203] van Paradijs J., McClintock J.E., 1995, Optical and ultraviolet observations of X-ray binaries. In: Lewin W.H.G., van Paradijs J., van den Heuvel E.P.J. (eds.) X-ray Binaries. Cambridge Univ. Press, p. 58
[204] Verbunt F., Belloni T., Johnston H.M., van der Klis M., Lewin W.H.G., 1994, A&A, 285, 903

[205] Vikhlinin A., Churazov E., Gilfanov M. et al., 1995, ApJ, 441, 779
[206] Wachmann A.A., 1948, Erg. Astron. Nachr., 11, E42
[207] Wagner R.M., Starrfield S.G., Howell S.B. et al., 1991, ApJ, 378, 293
[208] Wagner R.M., Kreidl T.J., Howell S.B., Starrfield S.G., 1992, ApJ, 401, L97
[209] Wallerstein G., 1992, Nat, 356, 569
[210] Watson M.G., 1976, MNRAS, 176, 19P
[211] Watson M.G., Ricketts M.J., Griffiths R.E., 1978, ApJ, L69
[212] Whelan J.A.J., Ward M.J., Allen D.A. et al., 1977, MNRAS, 180, 657
[213] Wilson C.K., Rothschild R.E., 1983, ApJ, 274, 71
[214] Wu C.-C., Aalders J.W.G., van Duinen R.J., Kester D., Wesselius P.R., 1976, A&A, 50, 445
[215] Yoshida K., Mitsuda K., Ebisawa K. et al., 1993, PASJ, 45, 605
[216] Zhang S.N., Wilson C.A., Harmon B.A. et al., 1994, IAU Circ. 6046
[217] Zhang S.N., Harmon B.A., Paciesas W.S., Fishman G.J., 1995, IAU Circ. 6209
[218] Zhang Z.-Y., Chen J.-S., 1992, A&A, 266, L9
[219] van Paradijs J., 1995, X-ray Binaries. In: Alpar M.A., Kizioglu Ü., van Paradijs J. (eds.) The Lives of the Neutron Stars. Kluwer Acad. Publ., Dordrecht, p. 281
[220] Kopal Z., 1978, Dynamics of close binary systems. Reidel Pub. Co., Dordrecht
[221] Verbunt F., van den Heuvel E.P.J., 1995, Formation and evolution of neutron stars and black holes in binaries. In: Lewin W.H.G., van Paradijs J., van den Heuvel E.P.J. (eds.) X-ray Binaries. Cambridge Univ. Press, Cambridge, p. 457
[222] van den Heuvel E.P.J., 1983, Formation and evolution of X-ray binaries. In: Lewin W.H.G., van den Heuvel E.P.J. (eds.) Accretion-driven stellar X-ray sources. Cambridge Univ. Press, Cambridge, p. 303
[223] Chen W., Livio M., Gehrels N., 1993, ApJ, 408, L5
[224] Mushotzky R.F., Fabian A.C., Iwasawa K. et al., 1995, MNRAS, 272, L9
[225] O'Donoghue D., Charles P.A., 1996, MNRAS, 282, 191
[226] Osaki Y., 1995, PASJ, 47, L11
[227] Osaki Y., 1995, PASJ, 47, L25
[228] Mineshige S., Hirose M., Osaki Y., 1992, PASJ, 44, L15
[229] Martín E.L., Spruit H.C., van Paradijs J., 1994, 291, L43
[230] Narayan R., Garcia M.R., McClintock J.E., 1997, ApJ, 478, L79
[231] Zhang S.N., Cui W., Chen W., 1997, ApJ 482, L155